Biogenesis and intercellular movement of Turnip Mosaic Virus replication vesicles

Camilo Patarroyo

Department of Biology

McGill University

Montreal, Quebec, Canada

2017

A thesis submitted to McGill University in partial fulfillment of the requirements of the degree of Master of Science

Table of contents	
LIST OF FIGURES AND TABLES	iv
ABREVIATIONS	vi
ACKNOWLEDGEMENTS	viii
CONTRIBUTIONS	ix
ABSTRACT	х
RÉSUMÉ	. xii
CHAPTER 1	1
INTRODUCTION AND LITERATURE REVIEW	1
1. Turnip Mosaic Virus	2
1.1 Taxonomy and genome organization	2
1.2 Turnip Mosaic Virus proteins	
1.2.1 6K2: the vesicle forming protein	
1.2.2 Proteins involved in the genome replication	
1.2.3 Proteins involved in the viral spread	
1.2.4 Proteins with not well characterized functions in the viral infection	
2. VESICLE TRANSPORT BETWEEN ER AND GOLGI	
2.1 COPII-mediated vesicle formation	
2.2 COPI-mediated vesicle formation	
3. POST-GOLGI VESICLE TRANSPORT	
4. PLASMODESMATA	
4.1 Plasmodesmal structure	
4.2 Plasmodesmata: size exclusion limit regulation	
4.3 Viral movement through plasmodesmata	
5. Yeast two hybrid – Split ubiquitin system	
6. RESEARCH OBJECTIVES	
6.1 Formation of 6K2 vesicles	
6.2 Minimum intercellular movement complex for TuMV replication complexes .	17
CHAPTER 2	
2.1 Introduction	
2.2 Results	
2.2.1 TuMV 6K2 interaction with Sec24	
2.2.2 Identification of Sec24-binding motif in TuMV 6K2	
2.2.3 Role of the binding of 6K2 to Sec24 in the formation of 6K2 vesicles	
2.2.4 Identification of the 6K2 recognition site in Sec24	
2.2.5 Role of the Sec24 recognition of 6K2 in the ER export of 6K2	
intercellular movement during TuMV infection	
2.3 Discussion	
2.3.1 Role of the COPII complex in the formation of TuMV replication vesicle	
	27

2.3.2 ER export motif of TuMV 6K2	29
2.4 Materials and methods	30
2.4.1 Plasmid construction and site directed mutagenesis	30
2.4.2 Transient protein expression	31
2.4.3 Infection assays in Arabidopsis thaliana	31
2.4.4 Coimmunoprecipitation and Western blot	31
2.4.5 Confocal microscopy	32
2.4.6 Yeast two hybrid assay	32
CHAPTER 3	42
3.1 Introduction	43
3.2 Results	44
3.2.1 CI and P3N-PIPO are necessary and sufficient to facilitate the intercellu	lar
movement of 6K2 vesicular bodies	44
3.2.2 CI and P3N-PIPO support the PD targeting of 6K2	
3.2.3 Targeting of P3N-PIPO to PD, but not the intracellular motility of 6l	
requires functional post-Golgi trafficking	
3.2.4 Inhibition of RabE1d-mediated post-Golgi transport affects PD targeting	of
6K2 vesicles	47
3.2.5 6K2 physically interacts to CI but not P3N-PIPO	48
3.2.6 Role of the interaction between CI and 6K2 in the intercellular movement	of
6K2 vesicles	49
3.3 Discussion	19
3.3.1 CI and P3N-PIPO compose the minimal complex required for t	he
intercellular movement of 6K2-vesicles	49
3.3.2 Infection-independent intercellular 6K2 vesicle movement assay	51
3.4 Materials and methods	
3.4.1 Plasmid construction and site directed mutagenesis	52
3.4.2 Transient expression in <i>Nicotiana benthamiana</i>	
3.4.3 Confocal microscopy	
3.4.4 Yeast tow-hybrid split-ubiquitin system	
CHAPTER 4	
Concluding statements and future directions	
4.1 Formation of TuMV replication vesicles	
4.2 Minimal viral complex for the intercellular movement of TuMV replicati	
vesicles	
REFERENCES	

List of Figures and Tables

Chapter 1:	
Figure 1: Schematic representation of the TuMV genome	18
Figure 2: Schematic representation of COPII-mediated vesicle formation	19
Figure 3: Schematic representation of COPI-mediated vesicle formation	20
Chapter 2:	
Figure 1: Interaction between 6K2 and COPII or COPI proteins	34
Figure 2: Co-Immunoprecipitation of YFP-Sec24 and 6K2-mCherry	34
Figure 3: Interaction between 6K2 N-terminal deletion mutants and Sec24	35
Figure 4: Interaction between 6K2 N-terminal point mutants and Sec24	35
Figure 5: Localization of 6K2 N-terminal point mutants fluorescently labeled w	ith GFP
	37
Figure 6: Interaction between 6K2 and point mutant Sec24(R693K)	38
Figure 7: Infection of a Sec24 mutant line by TuMV	39
Table 1: Primer table	41
Chapter 3: Figure 1: Intercellular movement of 6K2-GFP when co-expressed with CI an PIPO	
Figure 2: Localization of 6K2-mCherry to PD when co-expressed with CI an PIPO	d/or P3N-
Figure 3: Localization of P3N-PIPO, CI and PCaP1 when co-expressed w	
RabE1d or the dominant negative RabE1d(NI)	
Figure 4: Localization of the PD markers PDLP1-GFP and PDCB1-mCherry	
expressed with either RabE1d or the dominant negative RabE1d(NI)	
Figure 5: Localization of 6K2-mCherry relative to ER and Golgi markers	
expressed with either RabE1d or the dominant negative RabE1d(NI)	
Figure 6: Properties of 6K2-mCherry induced vesicles when co-expressed w	
RabE1d or the dominant negative RabE1d(NI)	
Figure 7: Localization of 6K2 to PD during TuMV infection when co-expression	
either RabE1d or the dominant negative RabE1d(NI)	
Figure 8: Interaction between 6K2 and either CI or P3N-PIPO	

Figure 9: Interaction between 6K2 and the CI point mutant CI(QS-124,126-AA)

Figure 10: Localization of CI point mutant when co-expressed with P3N-	
PIPO	
Figure 11: Intercellular movement of 6K2-mCherry when co-expressed with P3N-PIPO	
and either CI or CI(QS-124,126-AA)	
Figure 12: Schematic representation of the proposed mechanism of the intercellular	
movement of TuMV replication vesicles	
Table 1: Primer table	

Abbreviations

+ssRNA: Positive single stranded RNA

3-AT: 3-amino-1,2,4-triazole ADP: Adenosine diphosphate ARF1: ADP-ribosylation factor 1

BFA: Brefeldin A

BiFC: Bi-molecular fluorescence complementation

CCV: Clathrin-coated vesicles CFP: Cyan fluorescent protein CI: Cylindrical inclusion CoIP: Co-immunoprecipitation

CoIP: Co-immunoprecipitation COPI: Coat protein complex I COPII: Coat protein complex II

CP: Coat protein

Cub: C-terminal portion of ubiquitin

DNA: Deoxyribonucleic acid Dpi: Days post-infiltration dsRNA: Double-stranded RNA

EE: Early endosome

eEF1A: Eukaryotic translation elongation factor 1A eIF4a: Eukaryotic translation initiation factor 4a

eIF4e(iso): Eukaryotic translation initiation factor 4e isoform

ER: Endoplasmatic reticulum

ERES: ER-export site

GAP: GTPase activating proteins GDP: Guanosine diphosphate GEF: Guanine exchange factor GTP: Guanosine triphosphate GTPase: Guanosine triphosphatase

HC-Pro: Helper compound-protease

His: Histidine

Hsc70-3: Heat shock cognate 70-3 protein

LatB: Latrunculin B LE: Late endosome

Leu: Leucine

MP: Movement protein MVB: Multi-vesicular bodies

NTPase: Nucleoside triphosphatase Nub: N-terminal portion of ubiquitin

NubG: N-terminal portion of ubiquitin where the isoleucine 13 is replaced by glycine

OD: Optical density

P3N-PIPO: P3-N-terminal-Pretty Interesting Potyviral Open reading frame

PABP-2: Poly-A binding protein 2

PCaP1: Plasma membrane-associated cation binding protein 1

PD: Plasmodesmata

PDCB1: Plasmodesmata callose-binding protein 1

PDLP1: Plasmodesmata-located protein 1

PLV: Protein A-Lex A-VP16 artificial transcription factor

PM: Plasma membrane

PVC: Pre-vacuolar compartments

RdRp: RNA-dependent RNA-polymerase

RE: Recycling endosome RNA: Ribonucleic acid

SC: Synthetic complete medium

SEL: Size exclusion limit

SNARE: soluble N-ethylmaleimide-sensitive-factor adaptor-protein receptors

SUS: Split-ubiquitin system TGN: Trans-Golgi network TMV: Tobacco Mosaic Virus

Trp: Tryptophan

TuMV: Turnip Mosaic Virus VRC: Viral replication complexes

WT: Wild type

Y2H: Yeast two-hybrid

YFP: Yellow fluorescent protein

Acknowledgements

I would like to gratefully acknowledge my Supervisor Dr. Hugo Zheng for his guidance and immense help in designing and executing my project, his continuous support and valuable feedback on my thesis, which made this work a reality. I would like to thank my Co-Supervisor Dr. Jean-François Laliberté for his valuable insights on this project, his feedback and help in performing the relevant experiments. I would also like to gratefully acknowledge my fellow present and past lab members, Dr. Xingyun Qi, Jiaqi Sun and Mi Zhang as well as my colleagues from Dr. Laliberté's lab Dr. Romain Grangeon, Maxime Agbeci, Jun Jiang and Juan Wan for their valuable feedback on my project and their help performing my experiments. I would also like to thank my supervisory committee Dr. Tamara Western and Dr. Chen Liang for their valuable advice and encouraging discussions throughout this project as well as for their help improving my presentation skills. Thanks also to the members of the Brown and Western labs Bronwen Forward, Lydiane Gaborieau and Veronique Brulé for their valuable comments on this project. I would also like to thank Dr. Elke Küster-Schöck for her teachings and immense help with the confocal microscopy. This work was funded by a discovery grant from the Natural Sciences and Engineering Research Council of Canada to my supervisor, Dr. Hugo Zheng.

Contributions

The work presented in this thesis was done by myself. The co-immunoprecipitation experiment (Chapter 2, Figure 2, page 35) was done in collaboration with Jun Jiang from Jean-François Laliberté's lab (INRS, Laval, QC). Dr. Hugo Zheng and Dr. Xingyun Qi from the Zheng laboratory introduced me to most basic lab techniques, equipments and taught me to plant, grow and harvest *Arabidopsis thaliana*. Jun Jiang, Dr. Romain Grangeon and Dr. Jean-François Laliberté taught me to plant, grow and harvest *Nicotiana benthamiana* and introduced me to the agroinfiltration technique for transient expression in *N. benthamiana*.

Dr. Elke Küster-Schöck and Dr. Hugo Zheng taught me how to use the confocal microscope and corresponding software I used to analyze several samples and to obtain several of the figures in this thesis.

Jiaqi Sun, Bronwen Forward, Lydiane Gaborieau and Dr. Tamara Western together with Dr. Hugo Zheng helped me with the troubleshooting of various experiments and the constant and important feedback about my experiments and results.

Abstract

In plant cells infected by the Turnip Mosaic Virus (TuMV), a member of the Potyviridae family, small motile endoplasmic reticulum (ER)-derived vesicles are formed. These vesicles carry the viral RNA towards the plasmodesmata for transport into adjacent non-infected cells. The viral transmembrane protein 6K2 is responsible for the formation of such vesicles. However, the precise mechanism by which these vesicles are formed, and how are these moved between adjoining cells remains unclear. In this study it was found that 6K2 interacts directly with the COPII protein Sec24a. It was shown that one of three known cargo recognition sites of Sec24a (B-site) is in charge of the recognition of 6K2. Additionally, the previously unknown dual Sec24a binding signal LxLxxxxWN was identified in the N-terminal region of 6K2. Correspondingly, the formation of 6K2-induced replication vesicles and intercellular movement of TuMV were severely delayed in an *Arabidopsis thaliana* mutant line defective in Sec24a and when the dual Sec24a-binding signal LxLxxxxWN in 6K2 is mutated.

To enhance our understanding of the mechanism of cell-to-cell movement of the 6K2-induced replication vesicles, the P3N-PIPO and the CI helicase, shown to be involved in the intercellular movement of TuMV, were studied. It was found that, only when expressed together, CI and P3N-PIPO are necessary and sufficient to facilitate the intercellular movement of the 6K2-induced vesicular bodies. Further examination revealed that CI and P3N-PIPO support the correct targeting of the 6K2 vesicles to the plasmodesmata. When the PD targeting of P3N-PIPO is inhibited, the PD targeting of 6K2, but not its intracellular motility is also disrupted. Moreover, it was shown by yeast two hybrid that 6K2 is able to physically interact with CI but not with P3N-PIPO. Since

P3N-PIPO directs the targeting of CI to the plasmodesmata, it was hypothesized that the CI protein serves as a connection between the P3N-PIPO protein in the plasmodesmata and the 6K2-induced replication vesicles. This was further supported by the finding that disrupting the interaction between 6K2 and CI completely abolished the cell-to-cell movement of 6K2 vesicles.

Résumé

Dans les cellules végétales infectées par le virus de la mosaïque du navet (TuMV), un membre de la famille des Potyviridae, des petites vésicules dérivées des réticulum endoplasmique motiles (ER) sont formées. Ces vésicules transportent l'ARN viral vers le plasmodesmata pour le transport dans les cellules non infectées adjacentes. La protéine virale transmembranaire 6K2 est responsable de la formation de telles vésicules. Cependant, le mécanisme précis par lequel ces vésicules sont formées, et comment sontils déplacés entre les cellules adjacentes reste incertain. Dans ce travail on a constaté que 6K2 interagit directement avec la protéine Sec24a COPII. Il a été montré que l'un des trois cargos sites de reconnaissance connus de Sec24a (site B) est en charge de la reconnaissance de 6K2. En outre, la signal précédemment inconnu Sec24a double de liaison LxLxxxxWN a été identifié dans la région N-terminale de 6K2.

Corrélativement, la formation de vésicules de réplication 6K2-induits et le mouvement intercellulaire de TuMV ont été gravement retardé dans une ligne de mutant d'*Arabidopsis thaliana* défecteuse en Sec24a et quand la Sec24a double de liaison LxLxxxxWN de 6K2 est muté.

Pour améliorer notre compréhension du mécanisme de déplacement de la réplication induite par 6K2 cellule à cellule vésicules, le P3N-PIPO et l'hélicase CI, révélés être impliqués dans le mouvement intercellulaire de TuMV, ont été étudiés. On a constaté que, seulement quand elle est exprimée en même temps, CI et P3N-PIPO sont nécessaires et suffisantes pour faciliter la circulation intercellulaire des corps vésiculaires induites par 6K2. Un examen plus approfondi a révélé que CI et P3N-PIPO soutien le ciblage correct des vésicules 6K2 à la plasmodesmes. Lorsque le ciblage des PD P3N-PIPO est inhibée,

le ciblage des PD 6K2, mais pas sa motilité intracellulaire est également perturbée. D'autre part, il a été démontré par deux hybrides de levure qui 6K2 est capable d'interagir physiquement avec CI, mais pas avec P3N-PIPO. Etant donné que P3N-PIPO dirige le ciblage de CI au plasmodesmes, il a été émis l'hypothèse que la protéine CI sert de liaison entre la protéine P3N-PIPO dans le plasmodesmes et les vésicules de réplication induite 6K2. Cela a été encore étayée par la constatation que la perturbation de l'interaction entre 6K2 et CI complètement aboli le mouvement des vésicules 6K2 cellule à cellule.

Chapter 1:

Introduction and literature review

1. TuMV

1.1 Taxonomy and Genome organization

Turnip Mosaic virus (TuMV) is a member of the Potyviridae family. It has a monopartite positive single-stranded RNA (+ssRNA) genome [1]. The TuMV infects a broad spectrum of plants of the *Brassica* genus including the economically important oil-seed rape (*B. napus* ssp. *oleifera*) [2, 3]. TuMV is transmitted among host plants in a non-persistent manner by over 80 different species of aphids during feeding [4].

The TuMV genome is covalently linked to the viral VPg protein at its 5' end and polyadenylated at its 3' end (Figure 1) [4]. Like other (+)ssRNA viruses, TuMV induces the rearrangement of the endomembrane system for the viral infection (reviewed in [5-8]); this makes TuMV a valuable model for studying the virus-host interaction.

1.2 TuMV proteins

The TuMV genome encodes 11 proteins, 10 of which are proteolytically cleaved from a single polyprotein by the P1 protease, helper component-proteinase (HC-Pro), and viral protein linked to the genome (VPg-Pro) proteases (Figure 1) and P3N-PIPO that is translated by a ribosomal frameshift [9-11]. There are three viral proteases in charge of the cleavage of the polyprotein: P1, HC-Pro and VPg-Pro (Figure 1). P1 cleaves between P1 and HC-Pro, HC-Pro cleaves between HC-Pro and P3, and VPg-Pro cleaves in the sites P3 – 6K1, 6K1 – CI helicase, CI – 6K2, 6K2 – VPg, VPg – Pro, Pro – RdRp and RdRp – CP [10-12] (Figure 1). During the proteolytic processing of the -6K2-VPg-Proregion, the intermediates 6K2-VPg-Pro and VPg-Pro are produced [13]. The 6K2 containing intermediate is involved in the remodeling of the endomembrane system as

discussed below [13, 14]. The VPg-Pro intermediate is, in part, responsible for the processing of the polyprotein [12].

The mature proteins encoded by the viral genome are P1, HC-Pro, P3, P3N-PIPO, 6K1, the CI helicase, 6K2, VPg, Pro, RdRp and CP [1, 9]. These proteins can be classified into 4 groups based on its involvement in the TuMV infectious process: proteins involved in the remodeling of the host endomembrane system (6K2), proteins involved in the viral replication (RdRp, VPg-Pro and CI), proteins involved in the intercellular movement of the viral replication complexes (P3N-PIPO, HC-Pro, CI and CP), and proteins with not well defined functions (P1, P3 and 6K1).

1.2.1 6K2: the vesicle forming protein

6K2 is a 6kDa type 2 transmembrane protein (with its N-terminal towards the cytosol and C-terminal towards the ER lumen) and it is the sole protein responsible for the TuMV-induced remodeling of the host endomembrane system [13, 14]. 6K2 induces the formation of at least two kinds of newly formed membranous structures: small ER derived vesicular bodies and a large perinuclear body [13, 15]. The large perinuclear body is an amalgamation of ER membranes, Golgi bodies, COPI and COPII markers. The small vesicular bodies have been shown to be formed from and recycled back to the large perinuclear body [15]. Upon infection, various host and viral proteins involved in both RNA replication and translation are relocated to the 6K2-induced vesicles [16].

The small 6K2-induced vesicles have been shown to be the site where viral genome replication takes place as evidenced by the presence of the viral RNA-dependent RNA-polymerase (RdRp), dsRNA (intermediate of the TuMV genome replication) and the

active synthesis of RNA in the 6K2-induced small vesicles (described in detail in the next section [16-18]).

Additionally, during TuMV infection, the host poly-A binding protein 2 (PABP-2), eukaryotic translation initiation factor 4e (eIF4e(iso)) and eukaryotic translation initiation factor 4a (eIF4a) are relocated to the small 6K2-induced replication vesicles [13, 18-20]. This evidence suggests that the translation of the viral genome is taking place in these small vesicular bodies. Additionally, it was shown that active protein synthesis happens in the 6K2 replication vesicles during TuMV infection [16]. Interestingly, it was also shown that the host protein heat shock cognate 70-3 protein (Hsc70-3) interacts with the viral RdRp in the 6K2-induced replication vesicles [17]. The Hsc70-3 protein is a cytosolic chaperone involved in protein folding, translocation and assembly [21, 22]. In the case of several other viruses, cellular chaperones (such as Hsc70-3) are required for efficient replication of the viral genome [17, 23-27].

The 6K2 replication vesicles act also as the vehicle for intra- and inter-cellular movement of TuMV [16, 28]. During TuMV infection, the 6K2 replication vesicles are formed from modified ER membranes in a COPI-COPII dependent manner and move along actin microfilaments towards the cell periphery eventually reaching and moving through PD [15, 16, 28, 29]. It has been shown that inhibiting the COPI-COPII transport by Brefeldin A treatment (a drug that inhibits the transport between ER and the Golgi apparatus [30]) or the expression of a dominant negative mutant of Sar1 (discussed below [29]) abolish the formation of the 6K2-induced replication vesicles [15, 29]. Additionally, the depolimerization of the actin filaments using Latrunculin B completely abolish the intracellular movement of the 6K2-induced replication vesicles [16, 31].

It was recently shown that the 6K2-induced replication vesicles serve as the vehicle for systemic movement from the infected tissue to the rest of the plant. Upon infection, the 6K2 coated replication vesicles were found both in the sieve elements in the phloem and the xylem vessels. Furthermore, dsRNA (an obligate intermediate of the TuMV RNA genome replication) and the viral RdRp were found to localize to the 6K2 vesicles in both the phloem sieve elements and the xylem vessels [32].

1.2.2 Proteins involved in the genome replication

The TuMV RdRp is the protein that replicates the viral RNA genome [33]. During the TuMV infection this protein localizes to the 6K2-induced vesicular bodies through its interaction with VPg-Pro protein precursor [17, 33, 34]. As mentioned above, in addition to the viral proteins VPg-Pro and RdRp, the host proteins poly-A binding protein 2 (PABP-2), eukaryotic translation elongation factor 1A (eEF1A) and the heat shock cognate protein 70-3 (Hsc70-3) are recruited to the 6K2-vesicles though its interaction with both RdRp and the VPg-Pro proteins [17, 35].

Apart from the RNA replication, RdRp is capable of uridylylating the viral VPg protein in a template independent manner. The urydylated VPg serves as a primer for the synthesis of the complementary strand to the viral genome [36]. This negative strand serves as a template for the synthesis of the positive strand RNA viral genome.

The potyviral CI protein was shown to have NTPase and helicase activities [37-40]. The most likely role for CI in the viral replication is to unwind the secondary structure of the viral RNA. This is supported by the fact that mutations affecting the conserved helicase motifs of CI either abolishes or drastically reduces the viral replication efficiency [41-43].

1.2.3 Proteins involved in the viral spread

It is generally accepted that plant viruses move form cell-to-cell through the cell plasmodesmata (PD) (reviewed in [44-47]) and then systemically through the vascular system of the host plant [48, 49]. Most viral genomes encode for at least one dedicated movement protein (MP) (reviewed in [50]) that is involved in the cell-to-cell movement of the virus. In the case of TuMV it has been shown that the proteins P3N-PIPO, CI, CP and HC-Pro are involved in different steps of the viral spread process.

P3N-PIPO localizes to the PD during infection and, although the exact mechanism has yet to be described, it has been shown to increase the size exclusion limit of the PD and facilitate its own intercellular movement, similarly to most classically defined viral MPs [51-53]. The correct localization of P3N-PIPO to the PD requires a functional COPII-COPI transport pathway. When cells expressing P3N-PIPO were treated with either a drug that blocks the transport between ER and Golgi (BFA) [30] or a dominant negative Sarl, a small GTPase involved in the formation of COPII transport vesicles ([54, 55] reviewed in detail in the next section), was co-expressed with P3N-PIPO, P3N-PIPO failed to localize to the PD [52]. In contrast when the cells expressing P3N-PIPO are treated with an actin-depolymerizing drug (LatB) [56, 57], the localization of P3N-PIPO was not affected [52]. Similarly when dominant negative myosin VIII and XI, molecular motors of the acto-myosin system involved in vesicular and organelle traffic [58], are coexpressed with P3N-PIPO, P3N-PIPO is still correctly localized to PD [52]. These results together indicate that the localization of P3N-PIPO to the PD depends on the ER-Golgi transport but not on the acto-myosin system. P3N-PIPO interacts with the host cation binding protein PCaP1 at the PD [51]. Because P3N-PIPO does not have a transmembrane protein or a membrane anchor, it is hypothesized that PCaP1 might mediate the targeting of P3N-PIPO to PD. The finding that the intercellular movement of TuMV is severely delayed when PCaP1 is mutated supports this hypothesis [51].

The CI helicase, in addition to its key role in the genome replication, is required for the efficient intercellular movement of potyviruses [41, 59, 60]. Interestingly, the targeting of CI to the PD by P3N-PIPO is most efficient when the relative amounts of both CI and P3N-PIPO are equal (1:1 ratio) and progressively less efficient when the relative amount of CI is increased (up to 10:1 ratios) [52]. The targeting of CI to PD is mediated by the P3N-PIPO in a dose-dependent manner [52]. The CI helicase is capable also of self-interaction through its N-terminal portion [59, 61].

Similarly to the CI helicase, HC-Pro is a multifunctional protein. The C-terminal portion of HC-Pro has a cysteine protease activity and it performs its own cleavage from the polyprotein [62, 63]. The N-terminal portion of the protein is involved in the aphid transmission of the virus. The HC-Pro protein mediates the retention of the virions in the aphid stylet by physically interacting with the N-terminal portion of the coat protein and attaching to the aphid's stylet [63-67]. This interaction is a key determinant of the transmission efficiency of the virus by the aphids [67-69]. Consequently, the ability of the HC-Pro proteins from different potyviruses to bind to the stylet of specific aphids is a key determinant of the vector specificity of the virus [64, 68, 69].

In addition to its protease activity and its role in the aphid transmission, the central region of HC-Pro has been shown to enhance the genome amplification of the virus and in the suppression of the virus-induced gene silencing plant response [63]. In this central domain of HC-Pro, there are two RNA-binding domains A and B [70] that are thought to

be involved in the protection of the viral RNA from degradation and the inhibition of the viral-induced gene silencing [71].

The coat protein is necessary for the viral assembly and it has also been shown to be involved in the intercellular virus spread [71]. Up to 2000 copies of the CP arrange in a helical conformation in the presence of RNA to form the viral capsid. The N- and C-terminal domains are exposed in the outer part of the particle and are required for the inter-subunit interactions involved in the initiation of the viral particle assembly [72]. Further study showed that this protein is involved in the cell-to-cell and long distance movement of the virus [73]; CP also localizes to the PD together with P3N-PIPO and CI upon infection [52].

In addition to its involvement in the formation of the viral particles and the viral spread during infection, CP plays a major role in the aphid transmission by binding to the HC-Pro protein, which, in turn, binds to the aphid stylet. The interaction occurs between the N-terminal portion of CP and the N-terminal domain of HC-Pro [67-69]. Because CP is the major component of the viral capsid, it is one of the main determinants of the transmission specificity from the aphid vectors [68, 69].

1.2.4 Proteins with not well characterized functions in the viral infection

The potyviral P1 is the protein localized at the N-terminus of the viral genome and it mediates its own cleavage from the polyprotein [11]. The proteolytic motif is located in the C-terminal portion of P1 and it is required for the viral infection. Mutations on the N-terminal portion of P1 had no effect on the virus viability [74]. Interestingly the proteolytic cleavage of P1 from HC-Pro is required for the viral viability, however, the protease activity of P1 on itself is not [74]. The absence of P1 causes reduced viral

replication and severely impaired intercellular movement [43]. These effects could be rescued in *trans* by infecting plants expressing P1 [75]. P1 has also a non-sequence-specific RNA-binding activity [76]. The mode of action of this protein however is not completely clear.

The P3 protein has been characterized as the main pathology determinant of the TuMV. It was shown that when the P3 proteins of the UK1 strain was inserted in the CDN1 strain, the CDN1 strain caused the typical symptoms described for the UK1 strain infection and vice versa. Additionally, this experiment showed that the recognition of the virus by host resistance genes was also exchanged. P3 is a major determinant of the host specificity [77]. The P3 protein localizes to the cylindrical inclusions caused by the CI helicase and the 6K2-induced VRCs [78, 79]. Furthermore, mutations that affect the proteolytic cleavage of P3 from the 6K1 protein reduce the viral accumulation and symptom development, even though it does not completely impair the virus viability [80]. It is possible then that P3 plays a role in the viral replication.

6K1 is a soluble protein that does not have a known function in the potyviral infection; however, the fully cleaved mature 6K1 can be detected during viral infection [81, 82].

2. Vesicle transport between ER and Golgi

The protein transport between the endoplasmic reticulum (ER) and the Golgi apparatus is regulated mainly by two protein complexes, COPI and COPII. COPII is involved in the formation of transport vesicles from the ER towards the Golgi apparatus (anterograde transport). On the other hand, COPI is involved in the formation of transport vesicles from the Golgi apparatus back to the ER (retrograde transport) [55, 83].

2.1 COPII-mediated vesicle formation

The COPII-dependent vesicle formation process can be divided in the recruitment of the pre-budding complex (composed of Sar1 and Sec23/24), the assembly of the protein coat and the disassembly of the protein coat [54, 83, 84]. The minimal protein complex required for the formation of the COPII vesicles include the small Sar1 GTPase, the ER membrane anchored guanine exchange factor (GEF) Sec12, and the Sec23/24 and Sec13/31 heterodimers. The assembly of the pre-budding COPII complex starts with the activation of Sar1 by Sec12; then active Sar1-GTP is recruited to the ER membrane. The place where the COPII pre-budding complex is recruited is called the ER-export sites (ERES) [54, 55]. The Sec23/24 heterodimer then is recruited to the ERES by the interaction between the Sec23 subunit and Sar1 and the interaction between the Sec24 subunit and the cargo proteins [54, 83, 85].

The recognition of the cargo proteins by Sec24 occurs by the interaction of the ER-export signals located in the cytosolic portion of the cargo proteins and the Sec24 binding pockets [54, 84-87]. To ensure the recognition of the diverse cargo proteins, Sec24 has three different characterized binding pockets (named A-, B- and C- sites) that recognize different types of ER-export signals [87]. The A-site is a hydrophobic pocket in charge of the recognition of the YxxxNPF motif [88]. Interestingly, there is little sequence conservation in the A-site of the Sec24 proteins among different species, which suggests the possibility that the recognition of ER-export signals in the A-site is structure-based instead of sequence-based [88]. The B-site binds to the LxxM/LE and the DxD/E diacidic motifs [87, 88]. The C-site has not been as well studied as the other sites. It specifically recognizes the cargo protein Sec22, however the ER-export signal of Sec22 has yet to be identified [88]. Other characterized ER-export signals recognized by Sec24

contain two contiguous hydrophobic residues (for example: FF, LL, IL, FY) [86]. Neither the A- or B- sites of Sec24 bind to these signals since mutations that disrupt the function of these sites did not affect the ER-export of proteins containing di-hydrophobic ER-export signals [26, 87].

The binding of this pre-budding complex to the ER membrane initiates the deformation of the ER membrane [54]. Then Sec13/31 coatomer is recruited to the ERES to form a cage over the pre-budding complex, which helps in the formation of the spherical vesicles (Figure 2). Sec23 and the Sec13/31 heterodimer strongly enhance the intrinsic Sar1 GTPase activity [89]. After the budding of the transport vesicle, the enhanced GTP hydrolysis of Sar1 causes this protein to dissociate from the vesicle. The dissociation of the Sec23/24 and Sec13/31 occurs at a slower rate than the dissociation of Sar1 [90]. After the protein coat has dissociated, the naked vesicle is able to be transported to, and fuse with the Golgi apparatus.

2.2 COPI-mediated vesicle formation

The COPI complex regulates the formation of transport vesicles from the Golgi apparatus to the ER in a similar fashion as COPII. The COPI contains two main sub-complexes: the γ -COP – δ -COP – ζ -COP – β -COP complex which constitutes the inner layer, and the α -COP – β -COP complex which composes the outer layer of the protein coat (Figure 3) [91]. The protein complex recruitment starts with the activation of the small GTPase Arf1 (ADP-ribosylation factor 1) by a Golgi anchored Arf1-GEF containing the Sec7-domain [92]. Then the two protein sub-complexes are recruited to the Golgi apparatus. In the COPI complex the α -COP, β -COP, γ -COP and δ -COP subunits are involved in the cargo selection through the recognition of the cytosolic Golgi export

signals [92]. In addition to the coatomer, Arf1-GTPase activating proteins (GAPs) bind also to the nascent vesicle. These proteins enhance the inherent GTPase activity of Arf1 and are involved in the dissociation of Arf1 and the coatomer from the newly formed transport vesicle [55, 92, 93].

3. Post-Golgi vesicle transport

After being transported to the Golgi apparatus, proteins and lipids are then transported to either the plasma membrane (PM) or the lysosome/vacuole. This anterograde transport is mediated by transport vesicles towards the PM or clathrin-coated vesicles (CCV) to the endosome and then the lysosome. In mammalian cells the proteins modified in the Golgi apparatus are first delivered to the trans-Golgi network (TGN) before being sorted and transported towards the PM or the lysosome/vacuole [94]. The anterograde protein transport are balanced by several CCV-mediated endocytic pathways [95, 96].

The endocytic transport pathway starts with the formation of clathrin-coated vesicles from the PM. These endocytic vesicles are then delivered to the early endosome (EE), a compartment marked by the presence of Rab5, a small GTPase needed for the fusion of CCVs to the EE [97, 98]. Once in the EE, proteins can either be recycled back to the PM via recycling endosome (RE) [99], or transported to the late endosome (LE) and then the lysosome. The protein recycling via the EE is thought to be regulated by the small Rab11 GTPase [99]. The maturation of the LE is believed to be mediated by the fusion of different EEs, which in turn is regulated by the Rab7 GTPase and LE-specific SNARE (soluble *N*-ethylmaleimide-sensitive-factor adaptor-protein receptors) proteins [98, 100]. Despite the abundant parallels the post-Golgi traffic in plant cells differ from that in mammalian cells. In plant cells the TGN was first thought to be absent, however recent

evidence suggests that the TGN is possibly a motile organelle derived from the Golgi apparatus [101-103]. The plant TGN can act as a sorting station releasing two types of transport vesicles: secretory vesicles heading towards the PM and cell wall (CW) [103-105] and CCVs that mediate the transport to the vacuoles [102]. Differently from mammalian cells, it has been shown that the TGN in plant cells can also function as an early endosome (EE) [101, 103]. Proteins in the TGN/EE can be either recycled back to the PM [106] or transported to the multi-vesicular bodies (MVB) or pre-vacuolar compartments (PVC); from the MVB/PVC proteins can be targeted to the lysosome for degradation [107]. The PVC is equivalent to the LE in animal cells [107]. Interestingly no RE has been identified in plant cells. In plant cells the TGN/EE is marked by the presence of different RabA proteins [102, 103, 105], homologs of the animal Rab11 GTPase. On the other hand, the MVB/PVC is marked by the RabF proteins [106], homologs of the Rab5 GTPase in animal cells.

The exact proteins involved in the formation of secretory vesicles directed towards the PM in plants are currently unknown, however some of the small RabE and RabA GTPases have been shown to play an important role in the traffic of transport vesicles to the PM [108-110]. The known RabA proteins are key regulators of different post-Golgi traffic pathways. The expression of dominant negative RabA4c and RabA6a disrupts the normal endocytosis from the PM [108]; whereas expressing a dominant negative version of the RabA1b protein was shown to disrupt the protein transport from the TGN/EE to the PM [108, 109]. Similarly, the RabE1d protein has been shown to be required for the correct transport from Golgi towards the PM. It was shown that the expression of a dominant negative RabE1d mutant caused the retention of a secreted GFP marker in the

ER, Golgi and the PVC but did not affect the correct localization of either Golgi or vacuolar markers [110].

4. Plasmodesmata

4.1 Plasmodesmal structure

The plasmodesmata (PD) are a fundamental part of the intercellular communication in plants. PDs are nanochannels that connect the plasma membrane, ER and cytoplasm of neighboring cells (reviewed in [53, 111]). The plasmodesmata consist of an aperture in the cell wall separating two adjoining cells covered by PM; in this channel there is a membranous tube that connects the ER of the neighboring cells called desmotubule. Additionally there are various globular proteins located between the PM and the desmotubule arranged in a helical fashion along the PD channel [111]. Although the size of the PD varies, the diameter of the channel has been estimated to be between 30-80nm [112, 113] and the estimated pore size is somewhere between 3-8nm [112, 114]. The PD pore size is dynamically regulated and can be increased in order to allow the passage of larger macromolecules (reviewed in [115]).

The intercellular transport through PD can occur in two ways depending on the size of the transported macromolecules, passive or active. Passive transport is the non-selective concentration gradient driven cell-to-cell transport of molecules that do not exceed the PD size exclusion limit (SEL), defined as the maximum size of the largest molecules that can freely diffuse through the PD. On the other hand, the active transport involves the recognition of the transported molecules (like small RNAs, proteins and viruses) and the subsequent increase of the PD SEL to allow its intercellular movement [44, 115].

4.2 Plasmodesmata: size exclusion limit regulation

The regulation of the SEL is mediated mainly by the deposition of the glucose polymer callose (β -1,3-glucan) at the neck of the PD channel. Increased concentration of callose at the neck of the PD reduces its SEL [116, 117], conversely reduced concentrations of callose increases the PD SEL [118]. The concentration of callose is regulated by the antagonistic action of two main kinds of enzymes: callose synthases and β -1,3-glucanases [116-121] which synthesize and degrade callose respectively.

4.3 Viral movement through PD

Most known plant viruses move from cell-to-cell through the PD (reviewed by [44-46, 122]). However even the naked viral genomes are too large to fit in unmodified PD. To overcome this limitation most known plant viral genomes encode for at least one movement protein (MP). The function of the viral MPs is to interact with the PD and modify its structure to allow the intercellular viral movement [122]. The viral MPs employ at least two main kinds of movement, tubule-guided and non-tubule-guided. Tubule-guided refers to the modification of the PD by the insertion of a tubule formed by the viral MP which results in the dilation of the PD pore [123, 124]. On the other hand, in the non-tubule-guided movement the viral MP interacts with the PD and increases its pore size using cellular machinery without assembling a novel structure [45]. This is the case for the tobacco mosaic virus (TMV) MP. The TMV MP has been shown to associate with cell wall pectin methylesterases, involved in the modulation of the cell wall pH, which affects its porosity [125, 126], and to increase the PD pore size during infection [127]. However, the precise mechanism by which the non-tubule-forming MP increase the PD pore size is unknown.

5. Yeast two hybrid split-ubiquitin system

The split-ubiquitin system (SUS) is a variation of the conventional yeast two hybrid system optimized to test the interaction between pairs of proteins when at least one of the proteins is membrane bound. The SUS is based on the observation that the N-terminal portion of ubiquitin (Nub) can reconstitute the functional full-length protein when coexpressed with the C-terminal portion (Cub). However, when the isoleucine 13 is replaced by glycine in the Nub (NubG) its affinity for Cub is reduced. In this case, a functional ubiquitin can be reconstituted only when the two halves are brought into close proximity by interacting proteins. Cub is fused to the artificial transcription factor PLV (proteinA-LexA-VP16). Once reconstituted, the ubiquitin is then recognized by ubiquitin-specific proteases that release PLV. The free PLV diffuses then into the nucleus activating various reporter genes including HIS3 (required for the synthesis of histidine) and lacZ (which encodes for β-galactosidase and produces a blue color in a medium supplemented with X-Gal) [128].

The yeast with an interacting pair of proteins will then be able to grow on a medium lacking tryptophan, leucine (selection markers for the transformation of the plasmids containing each protein) and histidine and will turn blue when a X-Gal overlay assay is performed. In contrast, yeasts with a non-interacting pair of proteins will be able to grow on a medium without tryptophan and leucine but not in the selective medium lacking histidine [128].

6. Research objectives

The overall objective of research is to identify and characterize factors involved in the biogenesis and transport of the replication vesicles of TuMV induced by the 6K2 protein.

This project is divided into two parts, first the identification of host factors involved in the formation of the 6K2-induced VRC formation, and second the identification of the minimal viral complex cell-to-cell movement complex of the TuMV.

6.1 Formation of 6K2-vesicles

The principal objectives of this part are:

- 1. Identify host proteins involved in the early secretory pathway that interact with the TuMV 6K2 protein.
- 2. Find the sites of 6K2 and the interacting host protein(s) involved in such interaction.
- 3. Characterize the role of the host proteins in the formation of the 6K2 replication vesicles.

6.2 Minimum intercellular movement complex for TuMV replication vesicles

6K2 vesicles are the replication site of the TuMV genome. These vesicles move intercellularly during the viral infection [28]. On the other hand, the proteins P3N-PIPO, CI and CP among others have been shown to be involved in the cell-to-cell spread of the TuMV, the mechanism of action of these proteins, and the link between them has not yet been described. The main objectives of this part of the project are:

- 1. Identify the viral proteins that are sufficient to facilitate the intercellular movement of the 6K2-induced replication vesicles.
- 2. Study the mechanism by which the minimal intercellular movement complex facilitates the cell-to-cell movement of the 6K2-vesicles.

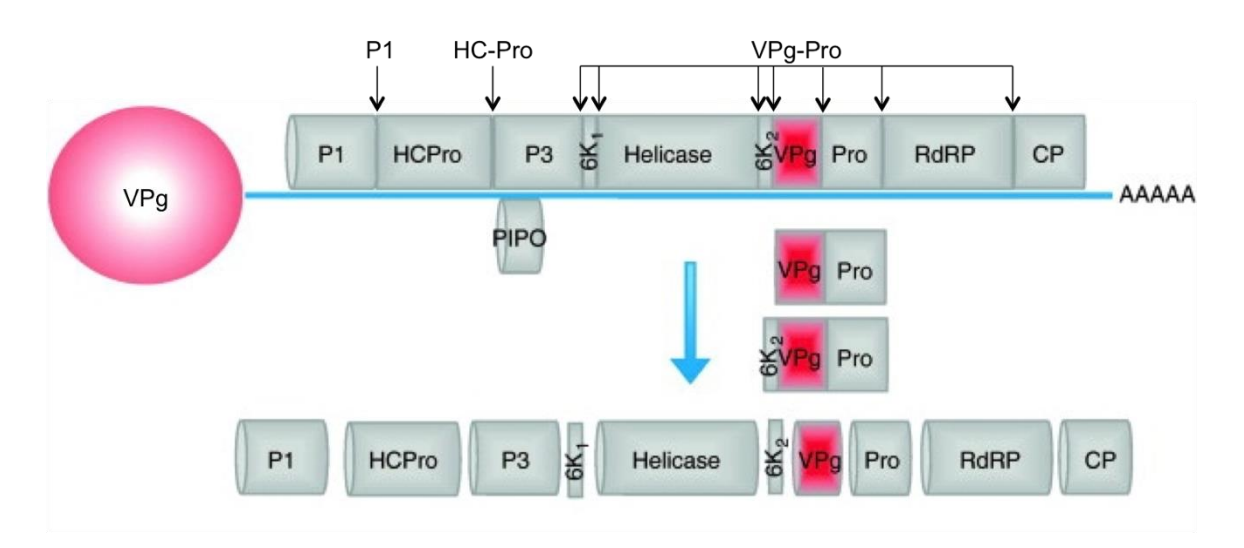


Figure 1: Genome organization of TuMV. The blue line represents the viral RNA covalently linked to the VPg protein at its 5' end (red circle) and polyadenylated at its 3' end. The polyprotein and the PIPO ORF are represented by gray squares. The proteases that cleave the polyprotein are shown above the ORF. The blue arrow represents the processing of the polyprotein into the mature proteins shown in the lower part. (Adapted from [129]).

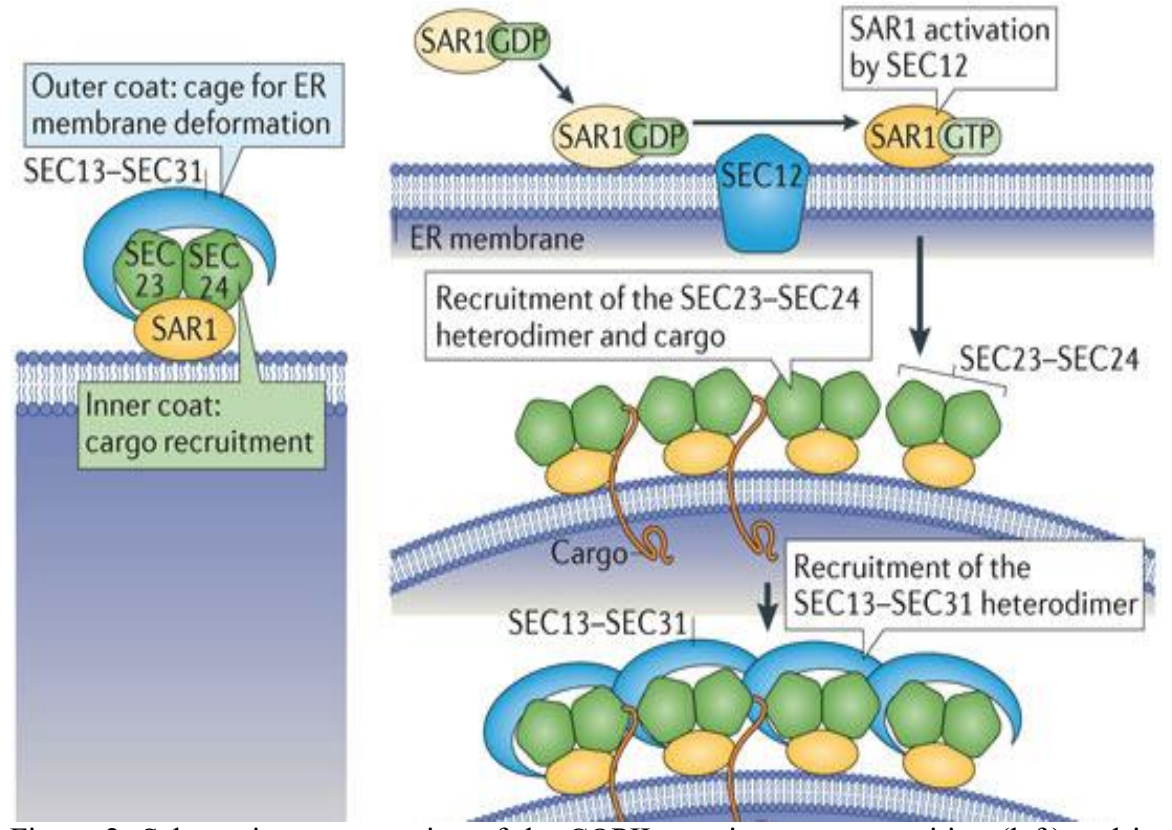


Figure 2: Schematic representation of the COPII protein coat composition (left) and its recruitment to the ER membrane (right). (Adapted from [55]).

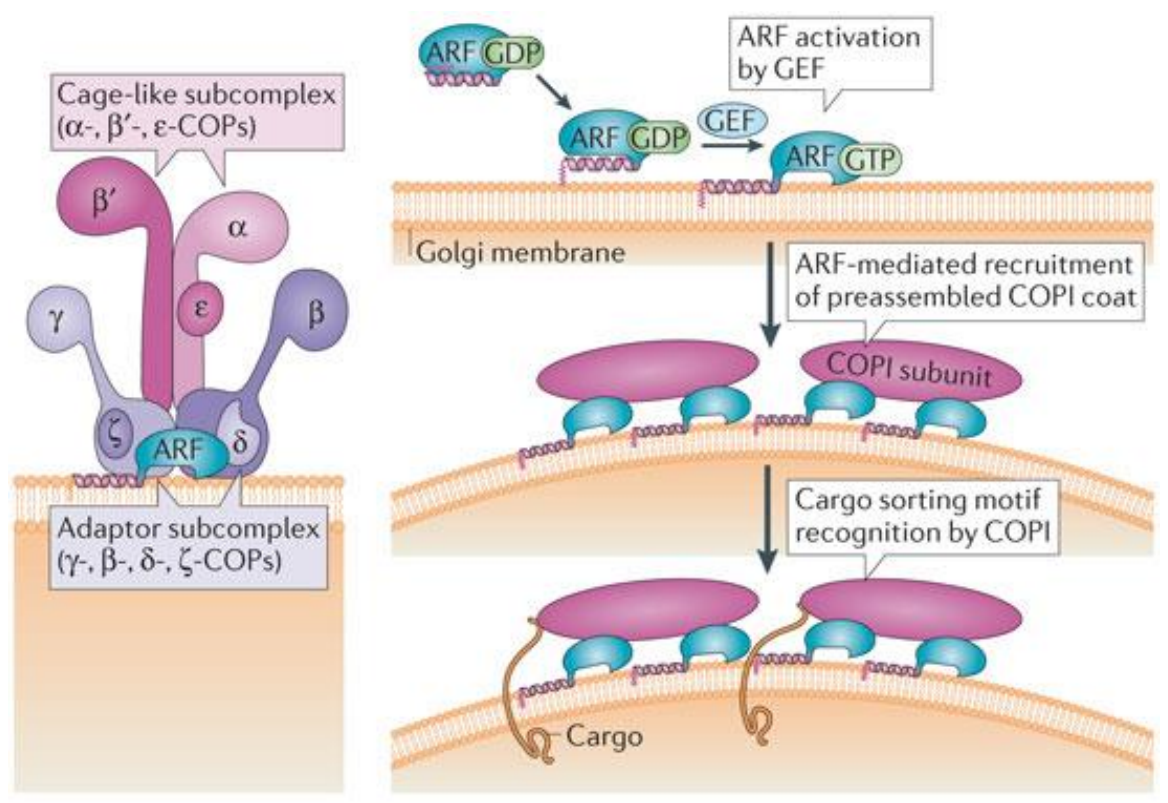


Figure 3: Schematic representation of the COPI protein coat composition (left) and its recruitment to the Golgi membrane (right). (Adapted from [55]).

Chapter 2:

6K2 protein of TuMV interacts with Sec24a for the formation of viral replication vesicles

2.1 Introduction

Previous studies have shown that the TuMV induces the rearrangement of the endomembrane system during infection as it has been described for several other (+ssRNA) viruses [5, 7, 15, 29, 130, 131]. TuMV forms two main kinds of morphologically different structures upon infection: a large perinuclear body and small punctaes [15]. The protein responsible for the formation of these structures is the transmembrane protein 6K2 [13]. These small vesicular bodies are known as the viral replication complexes (VRCs) because these are the site of the genomic replication and protein translation [16, 17, 19]. Additionally 6K2-induced vesicles are the vehicle for cell-to-cell movement during TuMV infection [28].

Interestingly, 6K2 alone is capable of inducing the formation of small vesicular bodies when ectopically expressed in plants [15, 81]. The formation of these vesicles is COPII-COPI dependent, which indicates that there are host factors involved in this process [29]. However, few of these host factors have been identified. In this chapter, *Arabidopsis* factors involved in the formation of COPII-COPI vesicles were screened for direct interaction with 6K2 using Y2H-SUS [128]. This screening led to the identification of 3 host proteins capable of interacting with 6K2. The protein Sec24a was chosen for further study for its involvement in the COPII-dependent export of ER cargo proteins [85, 87, 88]. The previously unknown ER export motif LxLxxxxWN was identified in the N-terminal portion of the TuMV 6K2 that interacts with the B-site of Sec24a. This interaction plays a determinant role in the formation of 6K2-induced viral replication complexes.

2.2 Results

2.2.1 TuMV 6K2 interaction with Sec24

The formation of transport vesicles for the transport between ER and the Golgi apparatus requires COPII and COPI (reviewed in [83, 132]). It is possible then that the formation of 6K2 vesicles requires the interaction of 6K2 with one or both complexes. To verify this possibility, the interaction between 6K2 and some of the proteins involved in the formation of COPII and COPI protein coats (γ-COP from COPI, and Sec24, Sec12 and Sar1 from COPII) was tested by Y2H. Since 6K2 is a transmembrane protein the SUS was used.

The yeasts containing PLV-Cub-6K2 and NubG-6K2 were used as a positive control (Figure 1) since the self-interaction of TuMV 6K2 has been shown by bi-molecular fluorescence complementation (BiFC) and co-immunoprecipitation (CoIP) [81]. The mated cells containing PLV-Cub-6K2 and an empty NubG vector were used as a self-cleavage control for the PLV transcription factor (as described in [128]) (Figure 1). PLV-Cub-6K2 interacted with NubG-Sec24, NubG-Sec12, and γ -COP-NubG, but not NubG-Sar1 (Figure 1).

It has been documented that the 6K2-coated VRCs are formed from ER-derived membranes [15]. Sec24 is the protein responsible for the cargo selection during the formation of COPII vesicles from the ER [85, 87, 88, 133]. One of the possibilities is that the 6K2 protein could act as a cargo protein to hijack the host COPII complex and induce the formation of the ER-derived vesicular bodies through the interaction of the viral 6K2 and the host Sec24. It has been shown that the formation of transport vesicles mediated by COPII for transmembrane cargo proteins requires a direct interaction between the coat

complex and said cargo [85, 87, 88]. Therefore, the interaction between the TuMV 6K2 and Sec24 was studied further.

To confirm this interaction in a plant system, the protein fusions 6K2-mCherry and YFP-Sec24 were transiently expressed in *N. benthamiana* and the interaction was assessed by co-immunoprecipitation of YFP-Sec24. 6K2-mCherry was specifically co-purified with YFP-Sec24 (Figure 2). Co-expression of free mCherry with either YFP-Sec24 or free YFP, and free YFP with 6K2-mCherry were used as negative controls (Figure 2).

2.2.2 Identification of Sec24-binding motif in TuMV 6K2

The next step in the investigation of the interaction between 6K2 and Sec24 was to determine the Sec24 binding motif of 6K2. Since 6K2 is a type 2 transmembrane protein with its N-terminus facing the cytosol and its C-terminus in the ER lumen [19] and the recognition of cargo proteins by Sec24 takes place in the cytoplasm (reviewed in [54, 83, 132]) it is possible that the Sec24 binding site of 6K2 is located in its N-terminal region. To find the region of 6K2 involved in this interaction, 3 deletion mutants of the N-terminal region of 6K2 were made (Δ 1-6, Δ 1-12, and Δ 1-18) and its interaction with Sec24 was tested by Y2H-SUS. The interaction of PLV-Cub-6K2 and NubG-Sec24 was used as a positive control (Figure 3). The interaction with NubG-Sec24 was maintained in the 6K2(Δ 1-6) and 6K2(Δ 1-12) mutants, but completely disrupted in the 6K2(Δ 1-18) mutant (Figure 3). This result suggests that the Sec24 binding signal of 6K2 is located in its N-terminal portion, likely, some residues in the 13-18 region (GKWNKT).

Classical COPII-mediated ER export signals found in transmembrane cargo proteins include di-acidic, di-hydrophobic and di-basic motifs ([87, 88, 134, 135] reviewed in [86, 136]). It is possible that the ER export signal of 6K2 resembles any of the previously

described motifs. Even though there are two lysine residues in the 13-18 region of 6K2, the di-basic motif was discarded because its ER-export is mediated through its direct interaction with the Sar1 protein [134, 137], and in the case of 6K2 there is no interaction to Sar1 (Figure 1). Because there are no acidic residues in the 13-18 region, the main residue of interest was the tryptophan in the 15th position. Interestingly there is a LxL motif in the positions 9-11 which is close to the previously described LL and LxxL motifs [86]. To determine if these motifs are sufficient to mediate the the interaction of 6K2 with Sec24, the point mutants 6K2(W15A) and 6K2(LLWN-9,11,15,16-AAAA) were made and its interaction with Sec24 was tested by Y2H-SUS. The PLV-Cub-6K2(W15A) mutant was still able to interact with NubG-Sec24, but the interaction between 6K2(LLWN-9,11,15,16-AAAA) and NubG-Sec24 was completely disrupted (Figure 4). This evidence suggests that this motif is necessary for the Sec24 recognition of 6K2.

2.2.3 Role of the binding of 6K2 to Sec24 in the formation of 6K2 vesicles

To determine the importance of the interaction between Sec24 and 6K2 in the formation of 6K2 vesicles, two alanine substitution mutations (WN-15,16-AA and LLWN-9,11,15,16-AAAA) were inserted in the 6K2-GFP fusion plasmid and the formation of 6K2 vesicles was observed. Either of the mutants or the wild type versions of 6K2-GFP were co-expressed with the ER-marker mCherry-HDEL and its localization was observed at 3dpi (Figure 5A) and at 5dpi for WT and the LLWN-9,11,15,16-AAAA mutant. The 6K2-GFP signal was only seen in small vesicular bodies that do not colocalize with the ER marker both at 3 and 5dpi as previously described (Figure 5) [15, 81, 138]. The signal of 6K2(WN-15,16-AA)-GFP at 3dpi was detected predominantly in small vesicular

bodies similarly to 6K2, but it showed a partial localization to the ER (Figure 5A) similarly to the 6K2(W-15-A)-GFP mutant [81]. The fluorescent signal of 6K2(LLWN-9,11,15,16-AAAA) co-localized strongly with the ER marker, and in some small vesicular bodies at 3dpi (Figure 5A). Interestingly at 5dpi 6K2(LLWN-9,11,15,16-AAAA) localized only to small vesicular bodies and it does not co-localize with the ER marker, just as 6K2-GFP (Figure 5B). This indicates that the formation of vesicles by 6K2(LLWN-9,11,15,16-AAAA) is severely delayed compared to the WT, but not completely disrupted.

2.2.4 Identification of the 6K2 recognition site in Sec24

As mentioned previously Sec24 has various different recognition sites that bind to different signals found in the cargo proteins [87, 88, 133]. Since the Sec24 binding signal found in 6K2 (LxLxxxxWN) is composed mainly of hydrophobic aminoacids it is possible that 6K2 binds to the B-site, which recognizes other proteins with hydrophobic ER export signals [88]. To test this hypothesis an R→K mutation was introduced in the position 693 of the NubG-Sec24 fusion and its interaction with PLV-Cub-6K2 was tested. This mutation corresponds to the R561 site of the yeast Sec24 that is part of the B-site binding pocket [88, 139] and partially affects the function of Sec24 [139]. NubG-Sec24(R693K) failed to interact with PLV-Cub-6K2. This result indicates that the 6K2 binds to the B-site of Sec24 (Figure 6).

2.2.5 Role of the Sec24 recognition of 6K2 in the ER export of 6K2 and intercellular movement during TuMV infection

To determine the role of the 6K2 recognition by Sec24 during the viral infection a construct containing an infectious clone of TuMV (with a copy of 6K2 fused to mCherry)

and the ER marker GFP-HDEL [138] was transfected into either a WT *Arabidopsis* Col-0 or an *Arabidopsis* line containing the R693K mutation in Sec24a (*g92* line) [139]. This dual construct has been used to monitor the intercellular movement of TuMV because the ER-marker (GFP-HDEL) cannot move from cell to cell, but 6K2-mCherry moves with the virus [138].

In the TuMV-infected WT *Arabidopsis* line at 6dpi, 6K2-mCherry localized to small vesicular bodies as seen for 6K2-GFP (Figure 5A) and a large globular structure (Figure 7A) as shown previously [138]. Additionally at this time there was intercellular movement of TuMV as evidenced by cells with mCherry but not GFP signal [138]. At later timepoints during infection (8 and 12dpi) there was an increase in the mCherry signal but there were no noticeable changes in the morphology of the 6K2-mCherry structures (Figure 7B and C).

The first thing to note in the infected *g92 Arabidopsis* line was the altered morphology of the ER (Figure 7D-F, arrowhead) that was similar to the previous characterization of this mutant line [139]. At 6dpi there was only a faint 6K2-mCherry signal that colocalized completely with GFP-HDEL (Figure 7D, arrow). At 8dpi the 6K2-mCherry signal was localized in small vesicular bodies similarly to the infection in the WT at 6dpi (Figure 7E). At this time, however there was no intercellular movement (Figure 7E). At 12dpi there was intercellular movement as in the infection of the WT line (Figure 7F).

2.3 Discussion

2.3.1 Role of the COPII complex in the replication vesicle formation of TuMV

Previous studies found that the formation of VRCs during potyviral infection requires a functional early secretory pathway [29]; however, the precise cellular machinery that is

hijacked during the viral infection and its role remained unknown. In the case of TuMV the protein in charge of the formation of these viral structures is 6K2 [13]. Through the interaction screening of 6K2 it was determined that there is a direct link between 6K2 and proteins from both COPI (γ -COP) and COPII (Sec24 and Sec12). Because the formation of the TuMV replication vesicles takes place from ER membranes [15] the vesicle formation of COPII is most likely to be hijacked to induce the formation of these structures.

Because Sec24 is a protein involved in the cargo selection of COPII [85, 87, 88], the interaction between Sec24 and 6K2 found by both Y2H-SUS and CoIP suggests the possibility that 6K2 could act as a cellular transmembrane cargo protein to hijack the COPII complex to induce the formation of small vesicular bodies. Interestingly when the interaction between Sec24 and 6K2 is disrupted by mutations in either 6K2 [in 6K2(LLWN-9,11,15,16-AAAA), Figure 5A] or Sec24 (in the g92 Arabidopsis line, Figure 7D-F) the ER export of 6K2 and subsequent formation of small vesicular bodies is delayed but not completely abolished. This means that even though the recognition of 6K2 by Sec24 plays a key role in its ER export, other mechanisms do exist. It is possible then that the binding of 6K2 with Sec12 could be sufficient to recruit the COPII complex to the ER membrane in a less efficient way. As previously mentioned the recruitment of the COPII complex is initiated by the recruitment of the pre-budding complex composed of Sec12, Sar1-GTP and the heterodimer Sec23/Sec24 [54, 83, 84]. Effective recruitment of the COPII complex depends on the stability of the association of the pre-budding complex to the ER membrane, which in turn depends on the activation of the small Sarl GTPase by Sec12 and the binding of Sec23/Sec24 to the cargo protein(s) mainly [90]. In the case of TuMV infection, 6K2 could efficiently recruit the COPII pre-budding complex directly by binding Sec24 and possibly by binding to Sec12 to increase the rate of Sar1 activation. It would be interesting to further investigate the precise nature and importance of the interaction between Sec12 and 6K2.

2.3.2 ER export motif of TuMV 6K2

Through progressive deletions of the N-terminal portion of the TuMV 6K2 protein and subsequent point mutations it was determined that the LxLxxxxWN motif is required for its binding to Sec24 and efficient ER export and subsequent formation of 6K2 vesicles (Figures 4 and 5). This signal resembles some of the di-hydrophobic signals found in other transmembrane cargo proteins ([88] reviewed in [86]). The ER export motif of 6K2 can be separated in two parts, LxL and WN. Interestingly either of these two motifs is sufficient to maintain the interaction of 6K2 with Sec24 as demonstrated by the interaction between Sec24 and either 6K2(Δ1-12) or 6K2(W-15-A) (Figures 3 and 4); however, when one of the parts is absent there is a partial arrest of 6K2 in the ER as shown by the 6K2(WN-15,16-AA)-GFP (Figure 5), 6K2(Δ1-12)-GFP and 6K2(W-15-A)-GFP mutant fusions [81], which indicates a less efficient ER export of 6K2. When both parts of the ER export motif in 6K2 are removed the efficiency of the ER export is severely reduced as evidence by the increased localization of the 6K2(LLWN-9,11,15,16-AAAA) (Figure 5) and 6K2(Δ1-18) mutants to the ER [81].

Together these results suggest the possibility that the dual ER-export motif found in 6K2 could have evolved to maximize the efficiency of the recruitment of Sec24, and hence the COPII complex, to the region of the ER where 6K2 is present. The increased recruitment

of COPII could lead then to a higher efficiency in the formation of 6K2-induced TuMV replication vesicles.

2.4 Materials and Methods

2.4.1 Plasmid construction and site directed mutagenesis

The coding sequence of 6K2 was amplified by PCR using the TuMV infectious clone [16] as template using the primers 6K2-F and 6K2-R (Table 1), and cloned into the pCR8 entry vector following the instructions from the manufacturer (ThermoFisher Scientific). The 6K2(Δ 1-6), 6K2(Δ 1-12) and 6K2(Δ 1-18) were amplified by PCR using the pCR8/6K2 vector as template with the primers 6K2(Δ 1-6)-F, 6K2(Δ 1-12)-F, 6K2(Δ 1-18) and 6K2-R (Table 1); the PCR products were then cloned into pCR8 (ThermoFisher Scientific).

RNA was extracted from 3-week old *Arabidopsis thaliana* using the RNeasy mini kit (Qiagen) and reverse transcribed using SuperScript III Reverse Transcriptase (ThermoFisher Scientific) with Oligo dT primers. The coding sequences for the Sec12, Sec24, Sar1 and γ-COP were amplified by PCR using the obtained cDNA as template and the corresponding primers (Table 1), and cloned into the pCR8 entry vector (ThermoFisher Scientific). All genes cloned into the pCR8 entry vectors were cloned into the corresponding Y2H gateway compatible vectors using LR clonase II plus enzyme mix (ThermoFisher Scientific).

The pCambia/6K2-GFP and the dual pCambiaTunos/6K2-mCherry/GFP-HDEL plasmids were kindly provided by Jean-François Laliberté; its construction was previously described in [17] and [138], respectively. The point mutations were generated with the

QuikChange Lightning kit (Agilent) following the manufacturer's instructions and using the corresponding primer pairs for each point mutation (Table 1).

2.4.2 Transient protein expression

The pCambia/6K2-GFP and mCherry-HDEL plasmids were provided in *Agrobacterium tumefaciens* AGL1 and GV3101 respectively. The pCambia/6K2(WN-15,16-AA)-GFP and pCambia/6K2(LLWN-9,11,15,16-AAAA)-GFP plasmids were transformed into *A. tumefaciens* GV3101 by using a modified freeze/thaw procedure [140]. The Agrobacterium containing the corresponding plasmids were grown in LB broth supplemented with kanamycin alone or kanamycin, gentamycin and rifampicin (for AGL1 or GV3101 respectively) overnight at 28°C with shaking. The cells were centrifuged at 2000g for 10 minutes and resuspended in infiltration buffer (10mM MgCl₂ and 150μM acetosyringone). The cell suspension was incubated for 4 hours at room temperature before infiltration. The OD₆₀₀ was measured for all cell suspensions and adjusted to 0.075. Agroinfiltration was done in 4 weeks old *Nicotiana benthamiana* plants as previously described [141].

2.4.3 Infection assays in *Arabidopsis thaliana*

Small abrasions were made in 4 weeks old *A. thaliana* leaves using sterile pipette tips, and the leaves were infiltrated with *Agrobacterium* containing the dual construct pCambiaTunos/6K2-mCherry/GFP-HDEL as described for *N. benthamiana* [141]. The *Agrobacterium* suspension's OD₆₀₀ was adjusted to 0.6.

2.4.4 Co-immunoprecipitation and Western blot

Approximately 0.3g of infiltrated *N. benthamiana* leaves (transiently expressing either YFP-Sec24, 6K2-mCherry or both) were harvested 3 days post-infiltration and ground to

powder in liquid nitrogen. Ground leaves were transferred to a tissue homogenizer and mixed with 3mL of immunoprecipitation buffer (50mM Tris [pH 7.5], 150mM NaCl, 10% glycerol, 0.1% Nonidet P-40, 5mM dithiothreitol, 1× Complete protease inhibitor cocktail [Roche]). Lysates were centrifuged at 20000 g for 15 min at 4°C. Then, 1mL of supernatant was incubated with GFP-Trap resin (Chromotek). The elution of the bound proteins was done as recommended by the manufacturer.

Protein samples were separated by SDS-PAGE in a 12% gel and transferred to a nitrocellulose membrane. Rabbit antisera were used at the following dilutions: anti-red fluorescent protein (anti-RFP) (Sigma) at 1:10000 and anti-GFP (Sigma) at 1:10000. The secondary antibody used was goat anti-rabbit IgG conjugated with horseradish peroxidase.

2.4.5 Confocal microscopy

Agroinfiltrated leaf sections were imaged using a Leica D6000 with the 40x immersion objective. Lasers were used to excite the fluorescent proteins and the capture of GFP and mCherry was done simultaneously. GFP was excited with a 488nm laser and its emission was captured at 500-540nm; mCherry was excited with a 561nm laser and the emission was captured at 580-620nm. Image processing was done in Image J (Rasband, W., http://rsbweb.nih.gov/ij/).

2.4.6 Yeast two-hybrid assay

The Y2H split-ubiquitin system (SUS) experiments were carried out as described by [128]. The THY-AP4 (MATa ura3 leu2 lexA::lacZ::trp1 lexA::HIS3 lexA::ADE2) and THY-AP5 (MAT32 URA3 leu2 trp1 his3 loxP::ade2) yeast strains were used. 6K2 was cloned in the bait vector pNCWTWRC1 to obtain the PLV-Cub-6K2 fusion protein, and

transformed into the THY-AP4 strain. 6K2, Sec12, Sec24 and Sar1 were cloned in the prey vector pNX32-DEST to obtain N-terminally fused NubG versions of these proteins. γ-COP was cloned into the prey vector pXN22 to obtain γ-COP-NubG. The prey vectors were transformed into the THY-AP5 strain. Lithium-acetate based transformation was used for all transformations as described in [128]. Following transformation THY-AP4 and THY-AP5 strains were mated and plated in SC-Leu-Trp. Mated cells were then plated in the SC-Leu-Trp-His plates supplemented with X-Gal and 1mM of the HIS3 competitive inhibitor 3-amino-1,2,4-triazole (3-AT) [142].

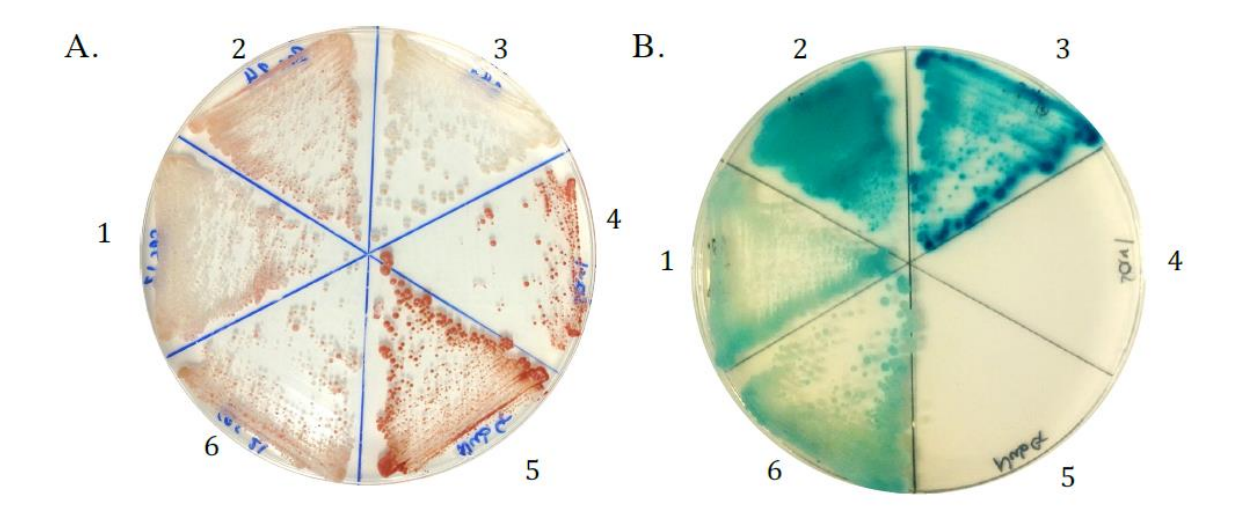


Figure 1: Y2H-SUS assay. Mated yeast cells expressing PLV-Cub-6K2 and NubG-Sec12 (1), NubG-Sec24 (2), NubG-6K2 (3), NubG-Sar1 (4), free NubG (5), and γ -COP-NubG (6). The mated cells were plated both in SC-Leu-Trp (A, mating control) and SC-Leu-Trp-His + 3-AT (B).

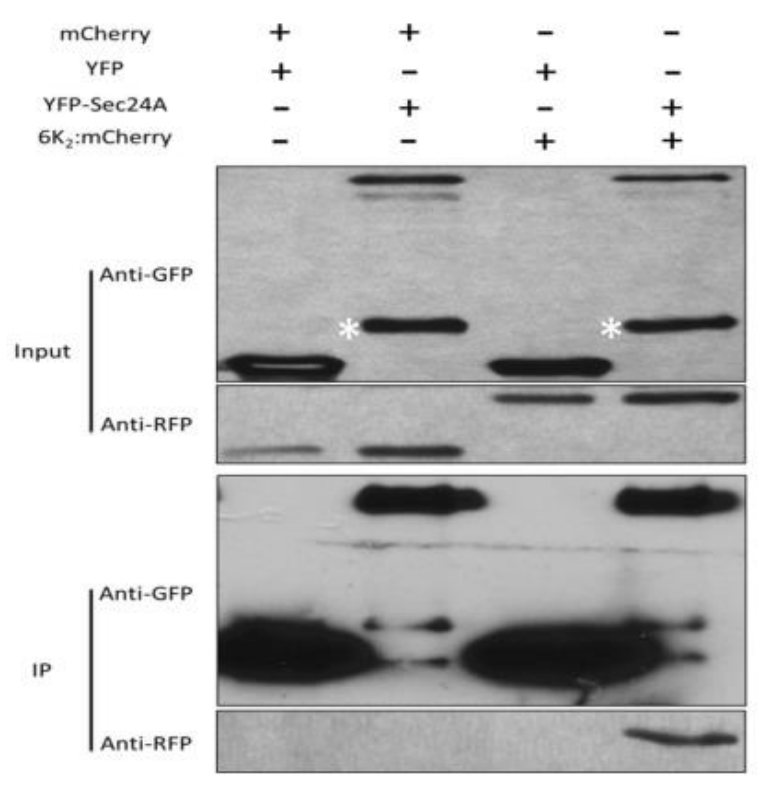


Figure 2: *N. benthamiana* leaves expressing combinations of mCherry, YFP, YFP-Sec24a and 6K2-mCherry as noted above were harvested 3 days after agroinfiltration (dpi). The lysates (input) were subjected to co-immunoprecipitation using a GFP-Trap resin followed by Western blot analysis of both the input and immunopurified (IP) fractions

using anti-GFP and anti-RFP antibodies. The asterisk indicates non-specific or a degradation protein species recognized by the anti-GFP antibodies.

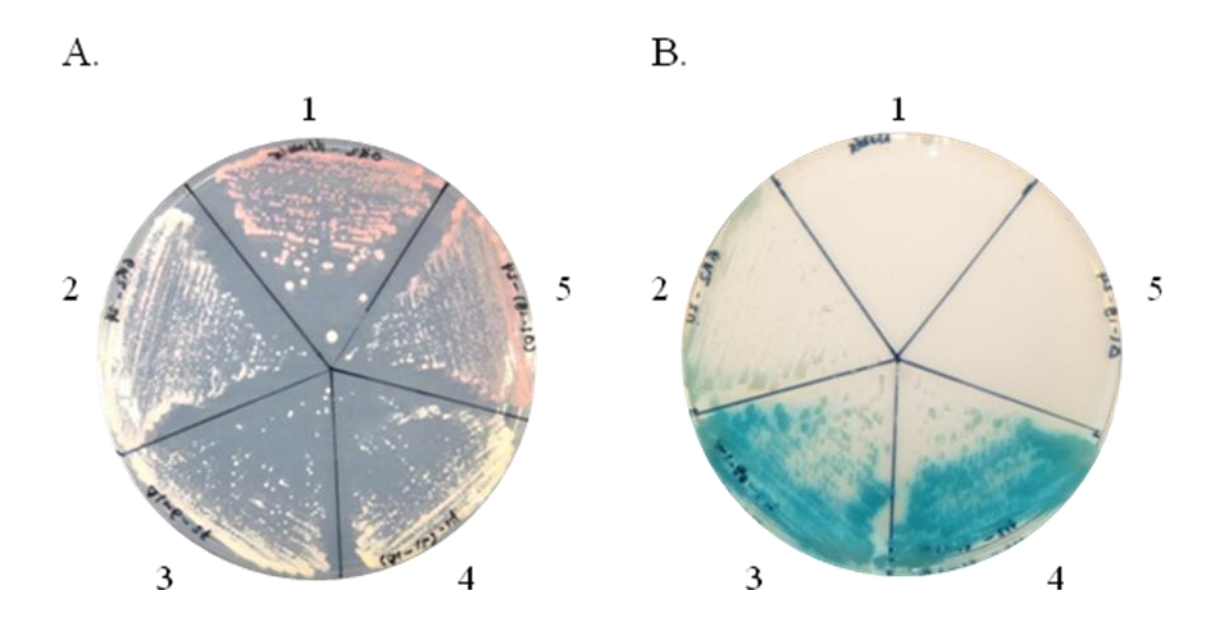


Figure 3: Y2H-SUS of the N-terminal deletion mutants of 6K2 and Sec24. Mated cells expressing PLV-Cub-6K2 and free NubG (1), PLV-Cub-6K2 and NubG-Sec24 (2), PLV-Cub-6K2(Δ 1-6) and NubG-Sec24 (3), PLV-Cub-6K2(Δ 1-12) and NubG-Sec24 (4), and PLV-Cub-6K2(Δ 1-18) and NubG-Sec24 (5) plated in SC-Leu-Trp (A, mating control) and in SC-Leu-Trp-His + 3-AT (B).

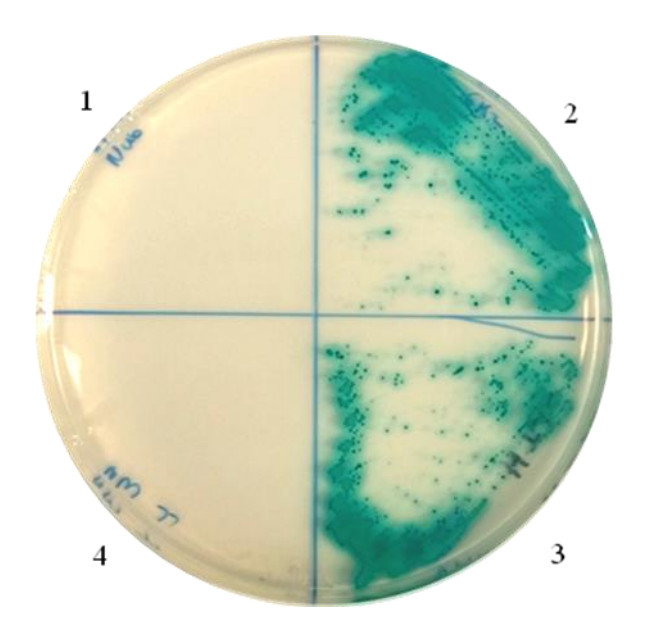


Figure 4: Y2H-SUS of the N-terminal point mutants of 6K2 and Sec24. Mated cells expressing PLV-Cub-6K2 and free NubG (1), PLV-Cub-6K2 and NubG-Sec24 (2), PLV-Cub-6K2(W-15-A) and NubG-Sec24 (3), and PLV-Cub-6K2(LLWN-9,11,15,16-AAAA) and NubG-Sec24 (4) in SC-Leu-Trp-His + 3-AT (B).

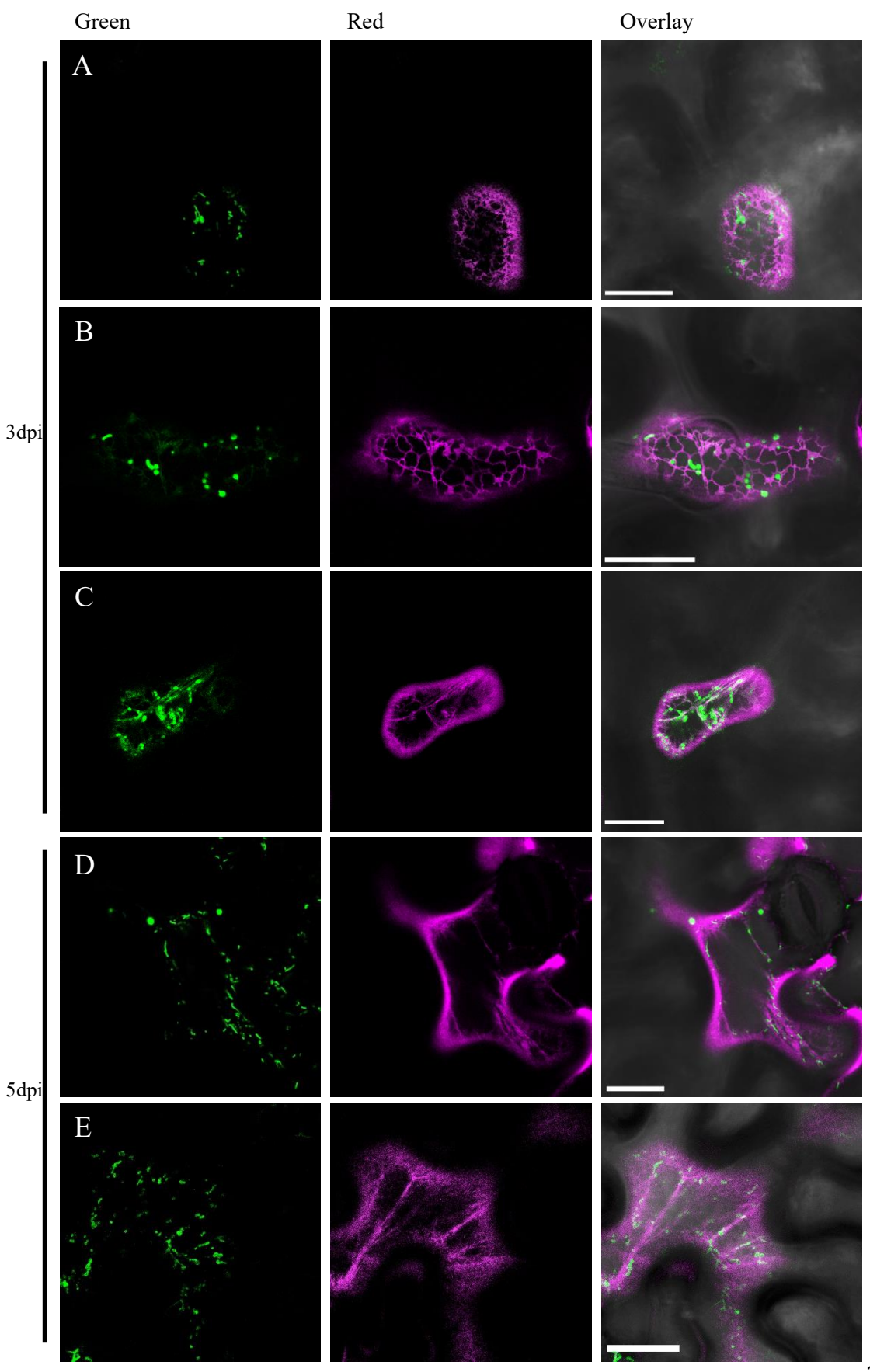


Figure 5: Localization of 6K2-GFP (A, D), 6K2(WN-15,16-AA)-GFP (B) and 6K2(LLWN-9,11,15,16-AAAA) (C, E) at either 3 or 5dpi. The ER marker mCherry-HDEL was co-expressed in all cases. GFP is shown in green and mCherry in magenta. Scale bar = $20\mu m$.

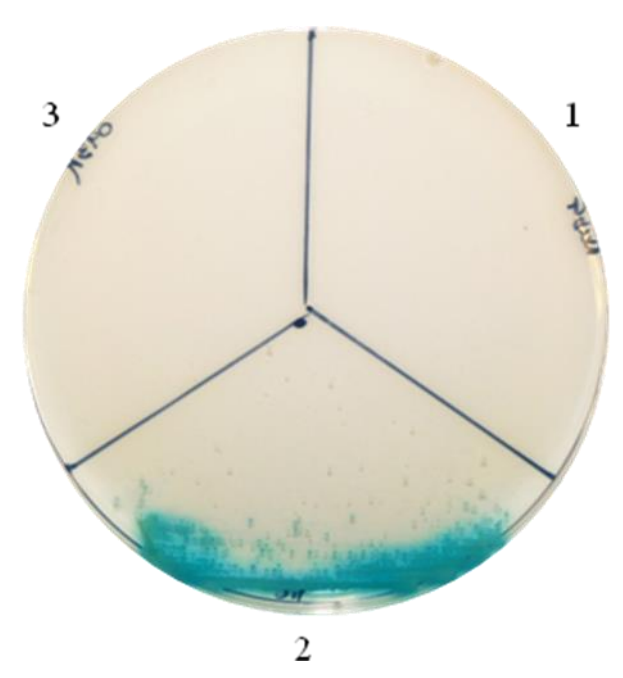


Figure 6: Y2H-SUS of PLV-Cub-6K2 and free NubG (1), PLV-Cub-6K2 and NubG-Sec24 (2), and PLV-Cub-6K2 and NubG-Sec24(R693K) (3). The mated cells containing both indicated plasmids were grown in the selective media SC-Leu-Trp-His + 3-AT.

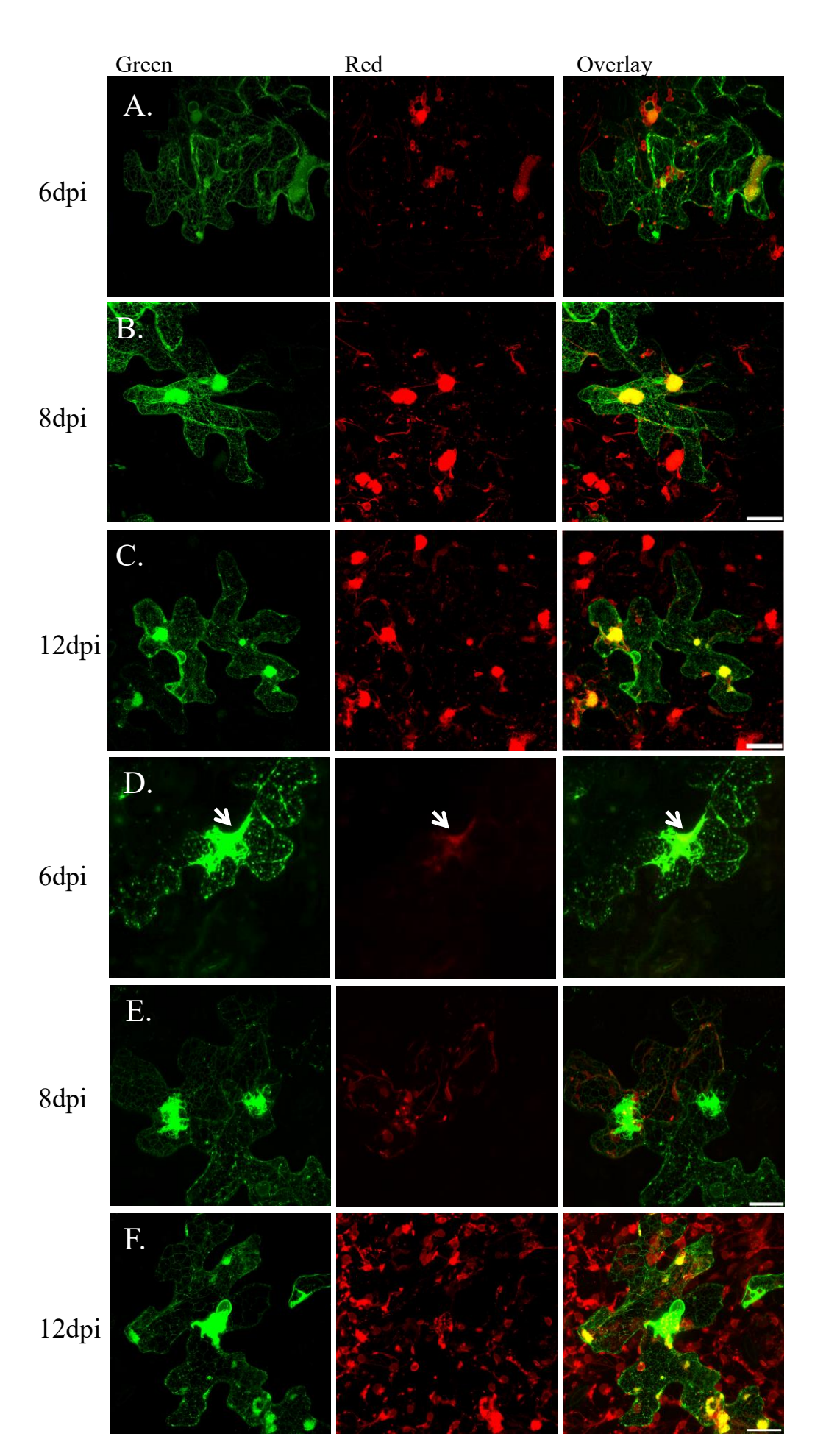


Figure 7: Infection of either *A. thaliana* Col-0 (WT) (A, B, C) or the *g92* mutant line (D, E, F) with the dual construct pCambiaTunos/6K2-mCherry/GFP-HDEL at 6, 8 and 12dpi. GFP and mCherry signal are shown in green and red correspondingly. Arrow: colocalization of 6K2-mCherry and GFP-HDEL.

Table 1: Primers used for the amplification and site directed mutagenesis of the genes used in this study.

Primer name	Sequence
Sec12-F	5' ATGCCGAATCAGAGTACAGAGACGA 3'
Sec12-R	5' TTCTAAGGTATGATACCCTTTGCCTTC 3'
Sar1-F	5' ATGITCTTGITCGATTGGITCTAC 3'
Sar1-R	5' TTAGTTGATGTACTGAGAGAGCCAT 3'
6K2-F	5' ATGAACACCAGCGACATGAGCAAATT 3'
6K2-R	5' TTCATGGGTTACGGGTTCGGACA 3'
6K2(Δ1-6)-F	5' ATGAAATTCCTCAAGCTTAAGGGC 3'
6K2(Δ1-12)-F	5' ATGGGCAAATGGAATAAAACGCTAATCACG 3'
6K2(Δ1-18)-F	5' CTAATCACGCGAGATGTGCTGG 3'
6K2(WN-15,16-AA)-F	5' CACATCTCGCGTGATTAGCGGTTTTAGCCGCTTTGCCCTTAAGCTTGAGGAATTTG 3'
6K2(WN-15,16-AA)-R	5' CAAATTCCTCAAGCTTAAGGGCAAAGCGGCTAAAACGCTAATCACGCGAGATGTG 3'
6K2(LL9,11AA)-F	5' GITTTATTCCATTTGCCCTTAGCCTTGGCGAATTTGCTCATGTCGCTGGTGTTCA 3'
6K2(LL9,11AA)-R	5' TGAACACCAGCGACATGAGCAAATTCGCCAAGGCTAAGGGCAAATGGAATAAAAC 3'
Sec24-F	5' TATCTCCTCCTATGTCTCTTCGC 3'
Sec24-R	5' AGCATTCCACTTTTAGTAGCCGA 3'
Sec24(R693K)-F	5' TCCTTTTCCACATTTTATTCGCATAACCGCCTCCC 3'
Sec24(R693K)-R	5' GGGAGGCGGTTATGCGAATAAAATGTGGAAAAGGA 3'
γ-COP-F	5' ATGGCGCAACCCCTCGTGAAGAAAG 3'
γ-COP-R	5' GCCGCTGGCAACAATCTCGTGA 3'

Chapter 3:

CI and P3N-PIPO of TuMV compose a minimal complex required for the intercellular movement of viral replication vesicles

3.1 Introduction

TuMV is a member of the potyviridae family [1]. It infects a broad spectrum of plants of the Brassica genus including the economically important oil-seed rape (B. napus ssp. *oleifera*). The genome of TuMV is monopartite positive single straded RNA ((+)ssRNA) that encodes for 11 different mature proteins [1, 9]. It has been shown that, upon infection, TuMV induces the rearrangement of the endomembrane system and the formation of small vesicular bodies through the transmembrane protein 6K2 [1, 15, 16, 19]. These small 6K2 vesicles are the site for the viral genomic replication and translation [16]; these vesicles can also serve as a vehicle for the cell-to-cell spread of TuMV [143]. The 6K2-induced replication vesicles traffic intracellularly along microfilaments and eventually reach the PD where these ultimately cross into the uninfected neighboring cell [16, 143]. Interestingly, even though the 6K2-induced vesicular bodies can be formed through the ectopic expression of 6K2, these are incapable of moving intercellularly [143], indicating that additional viral proteins are required for its intercellular movement. It is commonly accepted that plant viruses spread intercellularly through the PD. However, viral particles are too large to pass through PD. Most plant viruses encode for at least one protein that increases the size exclusion limit (SEL) of the plasmodesmata (PD) to allow the passage of viral particles from cell to cell [44, 45, 144-146]. In TuMV there are at least 3 proteins involved in viral cell-to-cell movement: P3N-PIPO, CI and CP. P3N-PIPO localizes to PD and modifies its size exclusion limit facilitating its own intercellular movement [51]. The CI helicase was shown to localize to PD in a P3N-PIPO-dependent fashion, where these proteins were shown to physically interact [52]. Mutations in the CI helicase outside of the conserved helicase domains from the related

potyvirus TEV severely delay or completely disrupt its intercellular movement [41, 52]. The CP also localizes to the PD together with CI and P3N-PIPO during TuMV infection [52]. Despite the study of the involvement of these proteins in the cell-to-cell movement of TuMV, the precise mechanism of action of CI, CP and P3N-PIPO in the cell-to-cell movement, or the connection between these PD-localized proteins and the 6K2-coated replication vesicles are still unknown.

In this chapter, the action of CI and P3N-PIPO in intercellular movement of 6K2-induced vesicular bodies is studied. We found that P3N-PIPO and CI are necessary and sufficient to facilitate the intercellular movement of the 6K2-vesicles. P3N-PIPO and CI are also sufficient to target the 6K2-vesicles to PD when expressed together. Additionally, 6K2 can physically interact with CI but not P3N-PIPO in a Y2H system. The evidence found suggests that CI could serve as a connection between the P3N-PIPO-modified PD and the 6K2-coated replication vesicles.

3.2 Results

3.2.1 CI and P3N-PIPO are necessary and sufficient to facilitate the intercellular movement of 6K2 vesicular bodies

P3N-PIPO alone is capable of increasing the SEL of the PD [51], and together with CI it accumulates at PD [52]. Furthermore, both proteins have been shown to play key roles in the intercellular spread of TuMV [41, 51, 52]. There is then a possibility that CI and P3N-PIPO could facilitate the intercellular movement of 6K2-vesicles in the absence of TuMV infection.

To test this, the dual construct pCambia/6K2-mCherry/GFP-HDEL [143] was expressed either alone, together with CI-YFP, P3N-PIPO-YFP or both. The intercellular movement

of 6K2-mCherry is seen as cells with only red fluorescence because the ER marker GFP-HDEL cannot move from cell to cell [143]. When the dual construct was expressed alone, or co-expressed with either CI-YFP or P3N-PIPO-YFP, there was no cell-to-cell movement of 6K2-mCherry (Figure 1A-C). Interestingly when the dual construct was co-expressed with both CI-YFP and P3N-PIPO-YFP there was intercellular movement of 6K2-mCherry (Figure 1D arrow). This indicated that both CI and P3N-PIPO are necessary and sufficient for the intercellular movement of 6K2-formed vesicular bodies. Further experiments were performed to clarify the mechanism by which P3N-PIPO and CI could facilitate the movement of 6K2-vesicles.

3.2.2 CI and P3N-PIPO support the PD targeting of 6K2

P3N-PIPO and CI are both localized to PDs when co-expressed, one of reasons why the presence of both proteins could facilitate the intercellular movement of 6K2 vesicles is that the presence of both proteins could support the PD targeting of 6K2. To verify this, the localization of 6K2-mCherry to PDLP1-GFP labeled PD was examined when co-expressed with P3N-PIPO, CI or both.

An apparent increase of the co-localization of 6K2-mCherry to PD was seen when both CI-CFP and P3N-PIPO-CFP were expressed together (Figure 2A-D). To confirm this result, the co-localization between 6K2-mCherry and PD was quantified during the ectopic expression of 6K2-mCherry, when co-expressed with CI-CFP and P3N-PIPO-CFP or during TuMV infection (Figure 2E). The co-localization between 6K2-mCherry and PDLP1-GFP was significantly higher when co-expressed with CI and P3N-PIPO when compared to the ectopic expression of 6K2-mCherry alone (Figure 2E). Interestingly the localization of 6K2-mCherry to PD was not significantly different either

during infection or co-expression with CI-CFP and P3N-PIPO-CFP (Figure 2E). These results suggest that these two proteins are sufficient to direct the 6K2-vesicles to PD.

3.2.3 Targeting of P3N-PIPO to PD, but not the intracellular motility of 6K2 requires functional post-Golgi trafficking

It has been previously described that the PD targeting of P3N-PIPO requires a functional COPII-COPI transport system but not actin microfilaments or myosin motors [52]. Additionally, the cation binding protein PCaP1 has also been shown to be involved in the targeting of P3N-PIPO to the PD [51]. The intracellular trafficking of 6K2-induced replication vesicles requires the COPII-COPI as well as actin microfilaments and myosin motors [16, 130]. We therefore wondered if the PD targeting of P3N-PIPO and intracellular motility of 6K2 take different intracellular pathways. To test this, a dominant negative mutant of the small GTPase RabE1d (RabE1d(NI)), a small GTPase involved in the post-Golgi trafficking towards plasma membrane [110, 147], which was shown to inhibit the intercellular movement of the virus but not its replication was used [138]. We first tested if the localization of the fluorescently labeled proteins CI-CFP and P3N-PIPO were altered when co-expressed the RabE1d(NI) dominant negative. Each of these fluorescent fusion proteins were co-expressed with either RabE1d or RabE1d(NI) and its localization was examined at 3dpi. The protein P3N-PIPO-CFP localized to PD when coexpressed with the WT version of RabE1d as previously described [52], but it showed a homogeneous distribution towards the plasma membrane when co-expressed with the RabE1d(NI) dominant negative (Figure 3A), suggesting that the PD targeting of P3N-PIPO requires a functional post-Golgi trafficking. Interestingly the localization of CI-CFP showed no noticeable differences when co-expressed either with the WT or the dominant negative version of RabE1d (Figure 3B, C). To verify the integrity of the general transport of cellular proteins to PD, the localization of PCaP1 and two PD markers was examined when co-expressed with either RabE1d or RabE1d(NI). The PD markers used were the transmembrane protein PDLP1-GFP [148] and the GPI-anchored protein PDCB1-mCherry [149]. There were no noticeable differences in the localization of either PCaP1-CFP, PDLP1-GFP or PDCB1-mCherry when co-expressed with RabE1d or RabE1d(NI) (Figure 4).

We next examined the formation or intracellular transport of 6K2-vesicles in the presence of either RabE1d or RabE1d(NI). 6K2-mCherry showed partial co-localization with GFP-HDEL only in the globular structure both when co-expressed with either RabE1d or RabE1d-(NI) (Figure 5A) as previously described [15]. Similarly, 6K2-mCherry did not co-localize with ST-GFP either when co-expressed with RabE1d or its dominant negative version (Figure 5B). To further study if the expression of RabE1d(NI) had any effect on the 6K2 vesicle formation or intracellular transport, the abundance, apparent size, speed of movement and localization to PD of 6K2-formed vesicular bodies were quantified when co-expressed with the dominant negative RabE1d(NI). There were no significant differences in the abundance (Figure 6A), apparent size (Figure 6B) and speed of movement (Figure 6C) of the 6K2 vesicles when co-expressed with RabE1d(NI) compared to RabEld. Taken all together, these results indicate that the formation and intracellular motility of 6K2 vesicles does not require a functional post-Golgi trafficking. 3.2.4. Inhibition of RabE1d-mediated post-Golgi transport affects PD targeting of 6K2 vesicles

Previously it was shown that the targeting of 6K2 to PD requires the presence of P3N-PIPO and CI (Figure 2E) and that the localization of CI to PD is mediated by P3N-PIPO [52]. Although the expression of the dominant negative RabEld(NI) does not disrupt the intracellular motility of 6K2 vesicles, it disrupts the correct localization of P3N-PIPO to PD (Figure 3A), therefore we wondered if the co-expression of RabEld(NI) would disrupt the targeting of 6K2-mCherry to PD. Since co-expressing 5 different constructs (P3N-PIPO, CI, 6K2, PDLP1 and either RabE1d or RabE1d(NI)) in the same cell is difficult, the effect of the co-expression of RabE1d(NI) in the PD targeting of 6K2vesicles was examined during TuMV infection. To test the targeting of 6K2-mCherry to PD, the co-localization of 6K2-mCherry and PDLP1-GFP was observed when coexpressed with either RabE1d or RabE1d(NI). There were no visible changes in the localization to PD of the 6K2-mCherry when co-expressed with either RabEld or RabE1d(NI) (Figure 7A, B); however, there is a significant decrease of the colocalization between 6K2-mCherry and PDLP1-GFP when the dominant negative RabE1d(NI) was expressed (Figure 7C). This evidence supports the idea that P3N-PIPO is a key determinant of the targeting of 6K2-vesicles to PD.

3.2.5 6K2 physically interacts to CI but not P3N-PIPO

Since P3N-PIPO and CI are sufficient to direct the PD targeting of 6K2-vesicles and its intercellular movement we wondered if 6K2 physically interacts with either of these proteins. The interactions between PLV-Cub-6K and either P3N-PIPO-NubG or CI-NubG were tested by Y2H-SUS. PLV-Cub-6K2 was found to interact with CI-NubG but not with P3N-PIPO in the Y2H-SUS system (Figure 8).

3.2.6 Role of the interaction between CI and 6K2 in the intercellular movement of 6K2 vesicles

In a previously reported screening, several mutants of the CI helicase from the potyvirus Tobacco Etch Virus (TEV) that delayed its intercellular movement were identified. One of the identified mutants presented severely delayed intercellular movement but showed no defects in the viral replication CI(RE-122,124-AA) [41]. The corresponding mutation (QS-124,126-AA) was introduced in the CI-NubG fusion plasmid and its interaction with PLV-Cub-6K2 was tested. CI(QS-124,126-AA)-NubG failed to interact with PLV-Cub-6K2 (Figure 9).

The QS-124,126-AA mutation was then introduced in the fluorescently labeled CI-YFP protein to make CI(QS-124,126-AA)-YFP and its localization was examined when coexpressed with P3N-PIPO-CFP. Both CI-YFP and CI(QS-124,126-AA)-YFP colocalized with P3N-PIPO-CFP at the PD (Figure 10).

Then we tested if the CI(QS-124,126-AA) mutant together with P3N-PIPO is capable of facilitating the intercellular movement of 6K2-vesicles. For this, the dual construct pCambia/6K2-mCherry/GFP-HDEL was co-expressed with P3N-PIPO-CFP and either CI-YFP or CI(QS-124,126-AA)-YFP and the cell-to-cell movement of 6K2-mCherry was evaluated. 6K2-mCherry was only able to move intercellularly when co-expressed with the CI-YFP but not with CI(QS-124,126-AA)-YFP (Figure 11).

3.3 Discussion

3.3.1 CI and P3N-PIPO compose a minimal complex required for the intercellular movement of 6K2-vesicles

It has been previously shown that the 6K2-induced replication vesicles are capable of moving intercellularly during TuMV infection. Even though 6K2 can induce the formation of these vesicular bodies when expressed ectopically, these 6K2 vesicles are incapable of moving from cell to cell [143].

We found that the viral proteins P3N-PIPO and CI are necessary and sufficient for the targeting of 6K2-vesicles to PD, and to facilitate the intercellular movement of 6K2vesicles during ectopic expression. We also found that 6K2 is capable of physically interacting with the CI protein but not P3N-PIPO in the Y2H-SUS; Also, the CI(QS-124,126-AA) mutant, which disrupts its interaction with 6K2, fails to support the intercellular movement of the 6K2-vesicles. P3N-PIPO localizes to the PD and it is capable of increasing its SEL [51]. During infection, CI localizes to PD through its interaction with P3N-PIPO [52]. Since 6K2 is capable of interacting physically with CI but not P3N-PIPO, these results suggest that CI could serve as the connection between the P3N-PIPO-modified PD and the 6K2-induced replication vesicles during infection. This is further supported by the finding that CI(QS-124,126-AA), even though it is localized to PD together with P3N-PIPO, is unable to facilitate the intercellular movement of the 6K2-vesicles. Moreover, although the intracellular transport of P3N-PIPO and the 6K2-vesicles depend on different host transport pathways, disrupting the PD localization of P3N-PIPO through the expression of RabE1d(NI) impairs the PD targeting of the 6K2-vesicles. This result indicates that P3N-PIPO is one of the key factors involved in the PD targeting of 6K2-vesicles.

Based on the result discussed above, the following model for the intercellular movement of TuMV replication vesicles is proposed: in a TuMV infected cell, upon successful replication, the P3N-PIPO protein is localized to PD, which requires the classic ER-to-Golgi transport pathways. the SEL of the PD is then increased by P3N-PIPO [51]. CI presumably localizes to the modified PD trhough its interaction with P3N-PIPO [52]. The 6K2-formed replication vesicles traffic along the actomyosin system towards the cell periphery eventually reaching the PD where the vesicles are docked to the P3N-PIPO-modified PD through the interaction between the 6K2 on the replication vesicle and the CI bound to P3N-PIPO. The PD-docked replication vesicles go through the PD into the neighboring cell [143] (Figure 12).

3.3.2 Infection-independent intercellular 6K2 vesicle movement assay

Previous studies on the regulation of the intercellular movement of potyviruses use infection assays [41, 51, 52, 59, 60]. This provides valuable information about the function of both viral and host factors involved in the intercellular movement of the viruses; however, the viral replication, and intra- and intercellular movement are linked during potyviral infection [41, 60, 68]. This makes the precise identification of the mechanism of action of host and viral proteins in the intercellular spread of the virus difficult.

In this chapter, an infection-free intercellular 6K2-vesicle movement assay is developed. Since there is no replication, the only process being observed is the cell-to-cell spread of the 6K2 vesicles. When combined with the expression of the dual construct pCambia/6K2-mCherry/GFP-HDEL [143] this system can be used to quantify the intercellular movement of 6K2 vesicles by measuring the amount of cells showing green and red fluorescence in comparison with the amount of cells showing red fluorescence only. With this system, the efficiency of this process could be accurately measured under

different experimental conditions. This could also prove to be a valuable tool in future studies about the precise mode of action of additional viral and host proteins involved in the intercellular spread of TuMV to form a more comprehensive model of the intra- and intercellular movement of this virus. One of the proteins of interest to be studied further is CP. This protein is located to the PD together with P3N-PIPO and CI [52], but its involvement in the cell-to-cell movement of replication vesicles is still not clear.

3.4 Materials and methods

3.4.1 Plasmid construction and site directed mutagenesis

The coding sequence of CI was amplified by PCR using the TuMV infectious clone [16] as template and the CI-F and CI-R primers (Table 1), and cloned into the pCR8 entry vector following the instructions from the manufacturer (ThermoFisher Scientific). The P3N-PIPO protein includes a +2 translational frameshift in the $G_{(2)}A_{(6)}$ motif. To mimic this shift an insertion of a G [9] in this motif (GGA AAA AA \rightarrow GGA AAG AAA) was done by PCR using the P3N-PIPO-F and P3N-PIPO-2-R, and the P3N-PIPO-2-F and P3N-PIPO-R (Table 1) to generate two overlapping pieces containing the G insertion, followed by an overlapping PCR combining both fragments and the P3N-PIPO-F and P3N-PIPO-R primers (Table 1). The full P3N-PIPO was then cloned into the PCR8 entry vector following the instructions from the manufacturer (ThermoFisher Scientific).

To clone the PCaP1 gene RNA was extracted from 3-week old *Arabidopsis thaliana* using the RNeasy mini kit (Qiagen) and reverse transcribed using SuperScript III Reverse Transcriptase (ThermoFisher Scientific) with Oligo dT primers. The coding sequence for the PCaP1 gene was amplified by PCR with the PCaP1 primer pair (Table 1) using the

obtained cDNA as template, and cloned into the pCR8 entry vector (ThermoFisher Scientific).

The CI gene cloned into pCR8 was cloned into pXN22-DEST [128] using LR clonase II plus enzyme mix (ThermoFisher Scientific) following the manufacturer's instructions to obtain the CI-NubG fusion. For the fluorescently labeled versions of these proteins, the three genes were cloned into the gateway compatible vectors pEarleyGate102 (X-CFP) to obtain the fluorescent fusion proteins P3N-PIPO-CFP, PCaP1-CFP and CI-CFP. P3N-PIPO and CI were additionally cloned into pEarleyGate101 (X-YFP) [150] using LR clonase II plus enzyme mix (ThermoFisher Scientific) to obtain CI-YFP and P3N-PIPO-YFP.

The pCambia/6K2-mCherry [81], the dual pCambia/6K2-mCherry/GFP-HDEL [143] and the PD markers PDLP1-GFP and PDCB1-mCherry [151, 152] were kindly provided by Jean-François Laliberté.

The point mutations of CI were generated with the QuikChange Lightning kit (Agilent) using the pEarleyGate101/CI-YFP and pXN22/CI-NubG plasmids as template to obtain the CI(QS-124,126-AA)-YFP and CI(QS-124,126-AA)-NubG protein fusions following the manufacturer's instructions using the primers indicated in Table 1.

The pVKHEn6-RabE1d and pVKHEn6-RabE1d(NI) plasmids were used for the expression of these proteins. The construction of these plasmids was described in [110].

3.4.2 Transient protein expression in *N. benthamiana*

The pCambia/6K2-mCherry, pCambia/6K2-mCherry/GFP-HDEL, pVKH-RabE1d and pVKH-RabE1d(NI) plasmids were provided in *A. tumefaciens*. The P3N-PIPO-YFP, P3N-PIPO-CFP, CI-YFP, CI-CFP and PCaP1-CFP plasmids were transformed into *A*.

tumefaciens by using a modified freeze/thaw procedure [140]. The *Agrobacterium* containing the corresponding plasmids were grown in LB broth supplemented with kanamycin alone (for pCambia/6K2-mCherry and pCambia/6K2-mCherry/GFP-HDEL, pVKH-RabE1d and pVKH-RabE1d(NI)) or kanamycin, gentamycin and rifampicin overnight at 28°C with shaking. The cells were centrifuged at 2000g for 10 minutes and resuspended in infiltration buffer (10mM MgCl2 and 150μM acetosyringone). The cell suspension was incubated for 4 hours at room temperature before infiltration. The OD600 was adjusted to 0.05 for the RabE1d and RabE1d(NI) containing strains as previously described [153] and to 0.1 for the rest since this concentration was found to yield a high efficiency of ectopic expression without causing adverse reactions in *N. bentamiana*. The agroinfiltration was done in 4 weeks old *N. benthamiana* plants as previously described [141].

3.4.3 Confocal microscopy

Agroinfiltrated leaf sections were imaged using a Leica D6000 with the 40x immersion objective at 3dpi. Lasers of 448nm, 488nm and 561nm were used to excite CFP, GFP and mCherry respectively. The capture was done at 460-480nm, 500-540nm and 580-620nm for CFP, GFP and mCherry. Image processing was done in Image J (Rasband, W., http://rsbweb.nih.gov/ij/).

The Pearson's correlation coefficient between the fluorescent signals was measured using the JACoP plug-in [154] in Image J.

To determine the abundance and size of the small vesicular bodies a stack was taken of individual cells expressing 6K2-mCherry, then the vesicles were counted using the 3D Object Counter plug-in in Image J using a size window of 10-1000 voxels.

To measure the average speed of the 6K2 vesicles a time-lapse was taken and the speed was measured in pixels per-timepoint using the MTrackJ plug-in [155] in Image J.

3.4.4 Yeast two-hybrid split-ubiquitin system assay

The Y2H-SUS experiments were carried out as described by [128]. The THY-AP4 (MATa ura3 leu2 lexA::lacZ::trp1 lexA::HIS3 lexA::ADE2) strain containing PLV-Cub-6K2 was used. CI-NubG and its mutant versions CI(RK-102,103-AA)-NubG or CI(QS-124,126-AA)-NubG transformed into the THY-AP5 (MAT55 URA3 leu2 trp1 his3 loxP::ade2) yeast strain. The transformation of the yeast strains was performed using a lithium-acetate based protocol [128]. Following transformation THY-AP4 and THY-AP5 strains were mated and plated in SC-Leu-Trp [128]. Mated cells were then plated in the SC-Leu-Trp-His plates supplemented with X-Gal and 1mM of the HIS3 competitive inhibitor 3-amino-1,2,4-triazole (3-AT) [142].

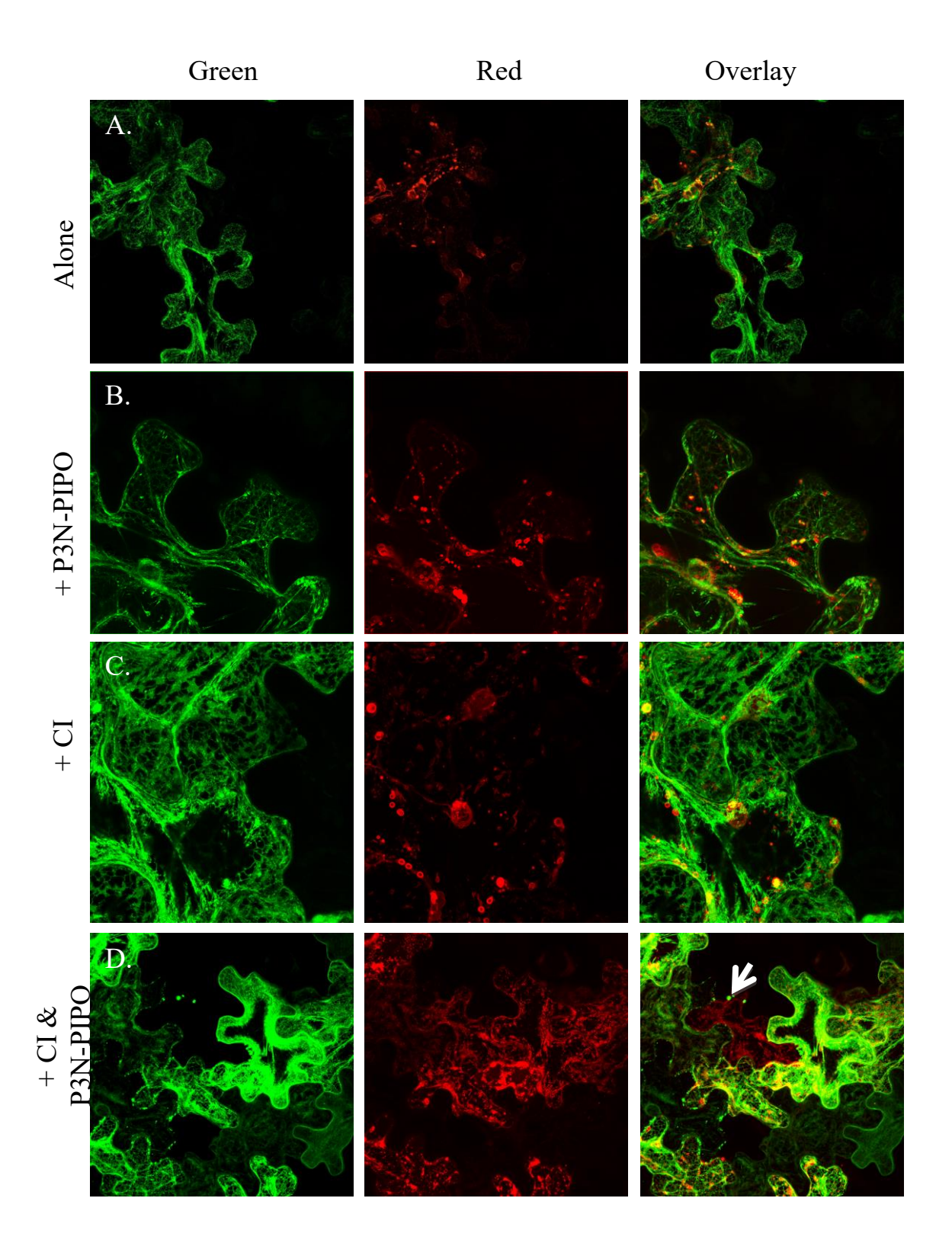
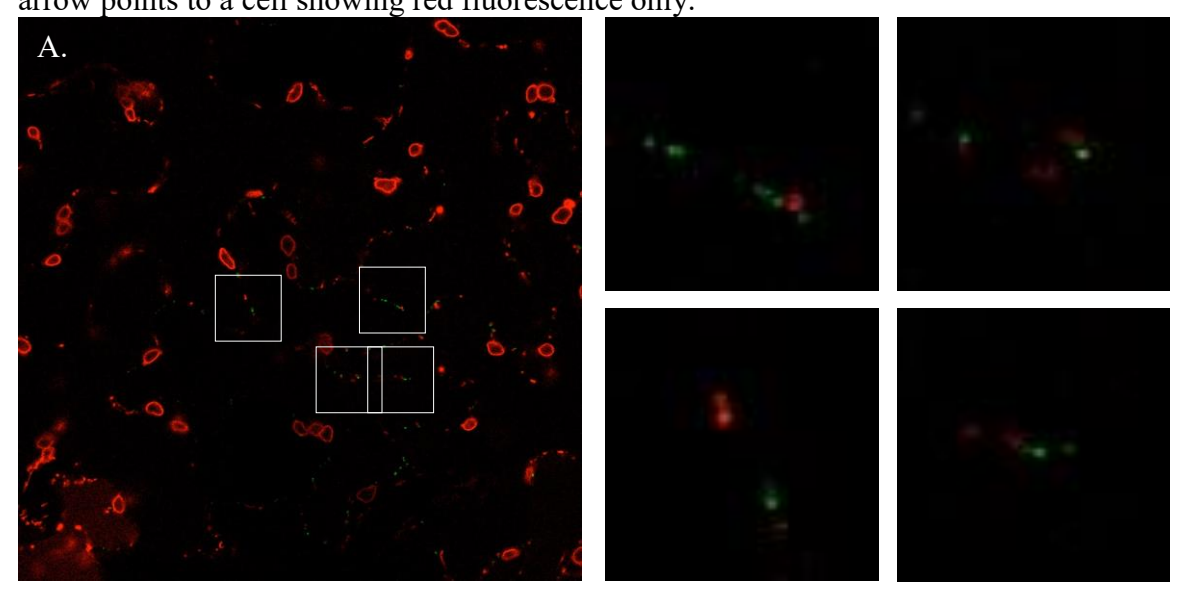
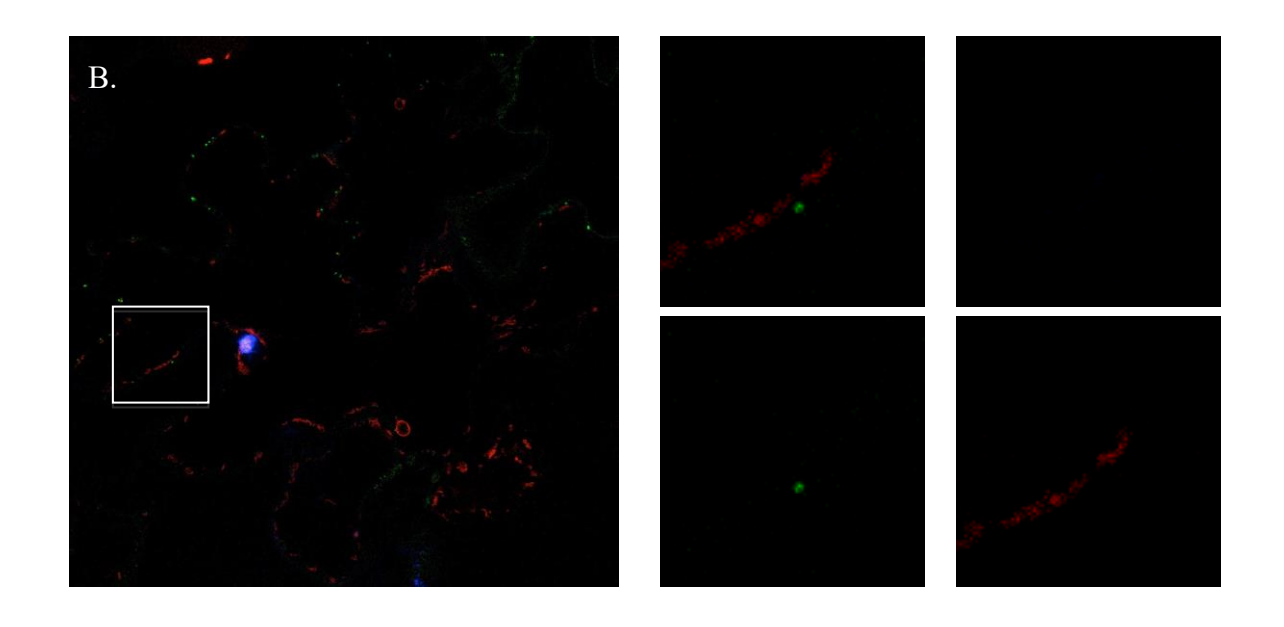
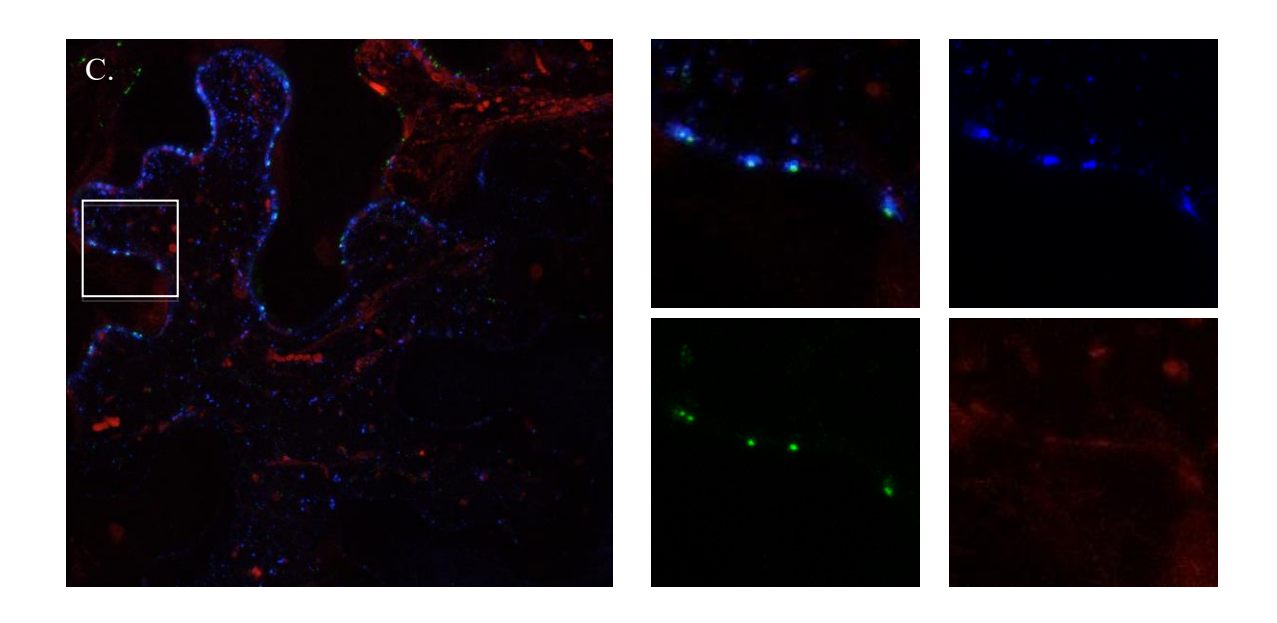
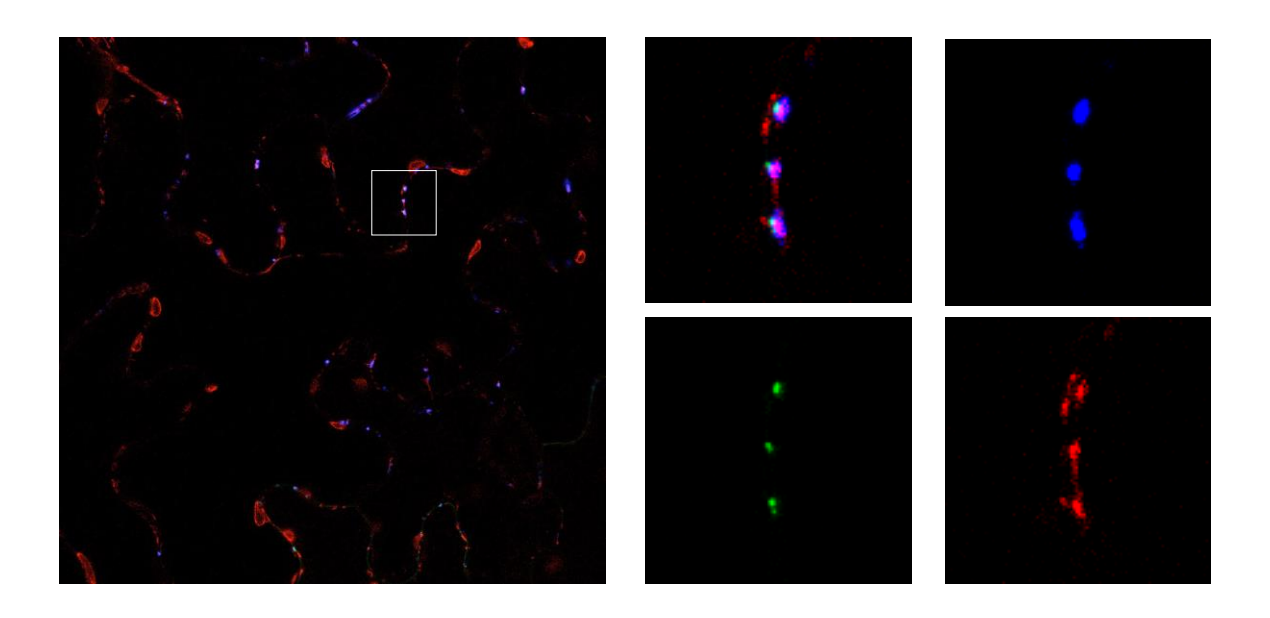


Figure 1: Expression of the dual construct pCambia/6K2-mCherry/GFP-HDEL alone (A), with P3N-PIPO-YFP (B), CI-YFP (C) or both CI-YFP and P3N-PIPO-YFP (D). White arrow points to a cell showing red fluorescence only.









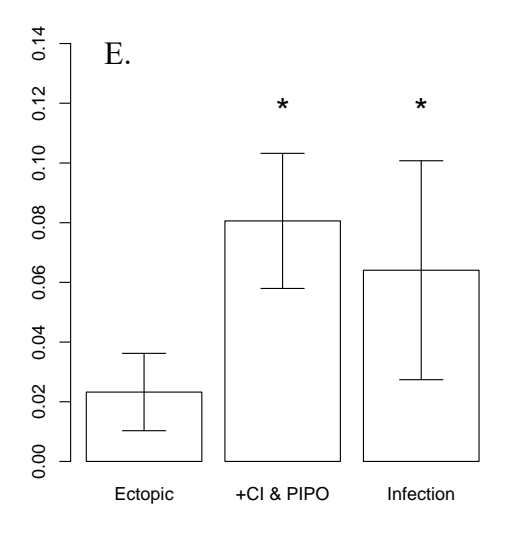


Figure 2: Localization of 6K2-mCherry to PDLP1-GFP labeled PD during ectopic expression either alone (A) or when co-expressed with CI-CFP (B), P3N-PIPO-CFP (C) or both CI-CFP and P3N-PIPO-CFP (D). Quantification of the co-localization (PCC) between 6K2-mCherry and PDLP1-GFP when expressed alone (Ectopic), when co-expressed with CI-CFP and P3N-PIPO-CFP or during infection (E) (t-test comparing either CI + P3N-PIPO or infection against ectopic expression of 6K2; n=20, p-value<0.05).

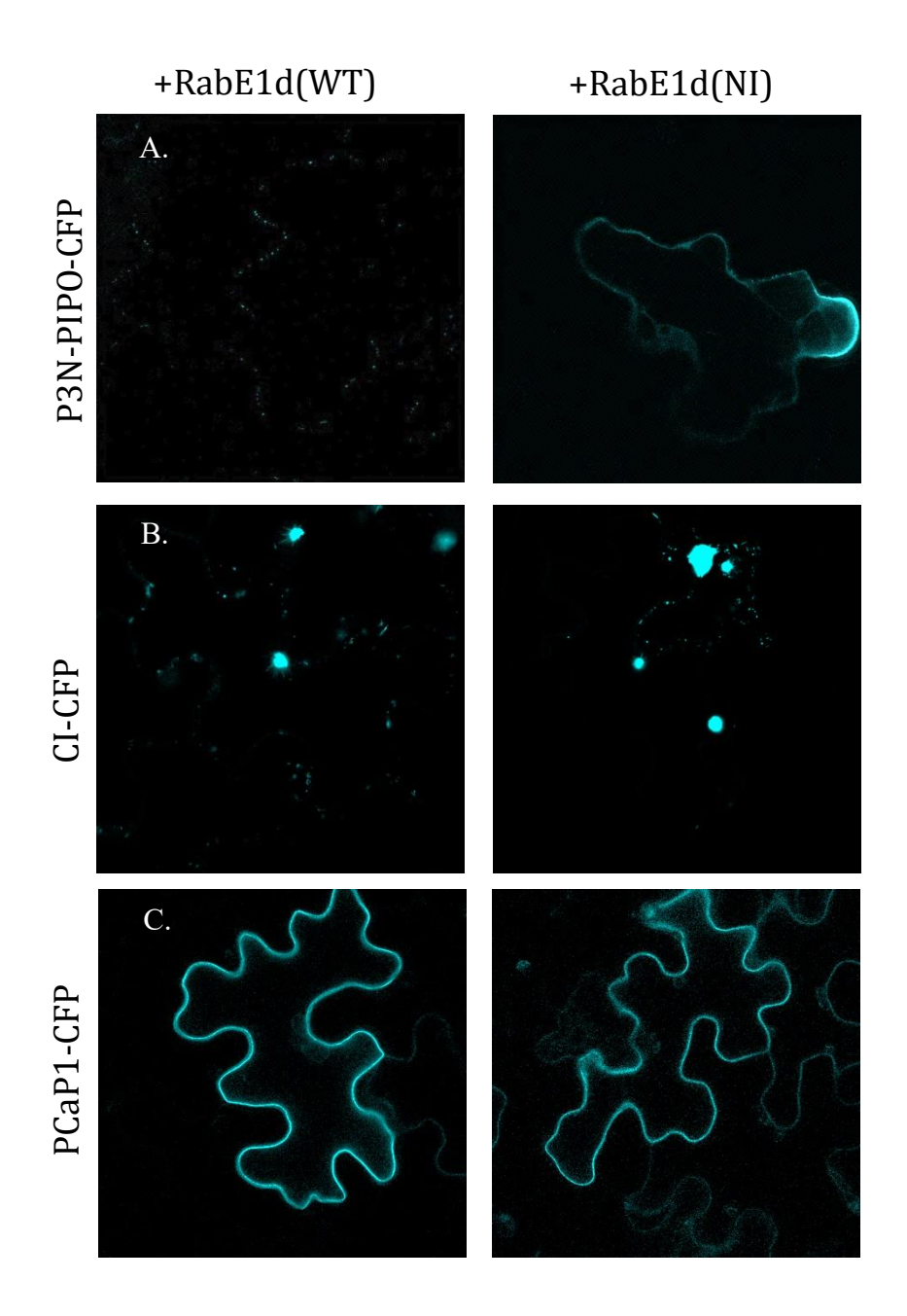


Figure 3: Localization of the proteins P3N-PIPO-CFP (A), CI-CFP (B) and PCaP1-CFP (C) when co-expressed with either RabE1d or the dominant negative RabE1d(NI).

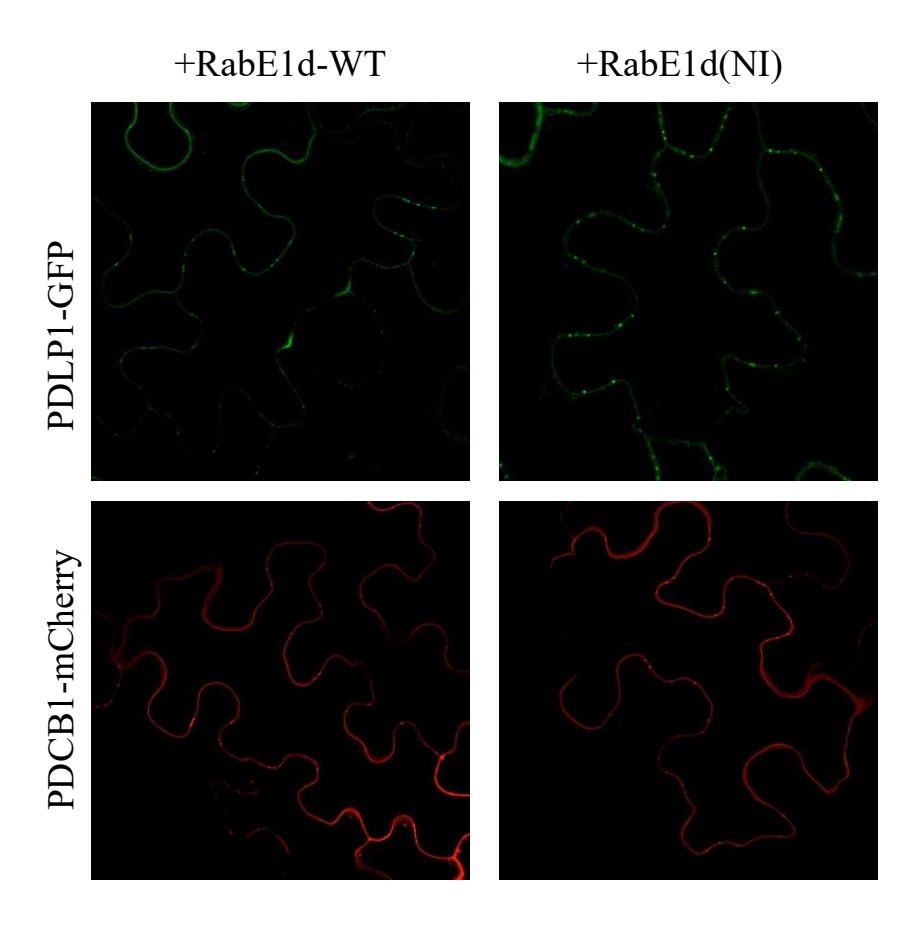


Figure 4: Localization of PDLP1-GFP (A) and PDCB1-mCherry (B) when co-expressed with either RabE1d or RabE1d(NI).

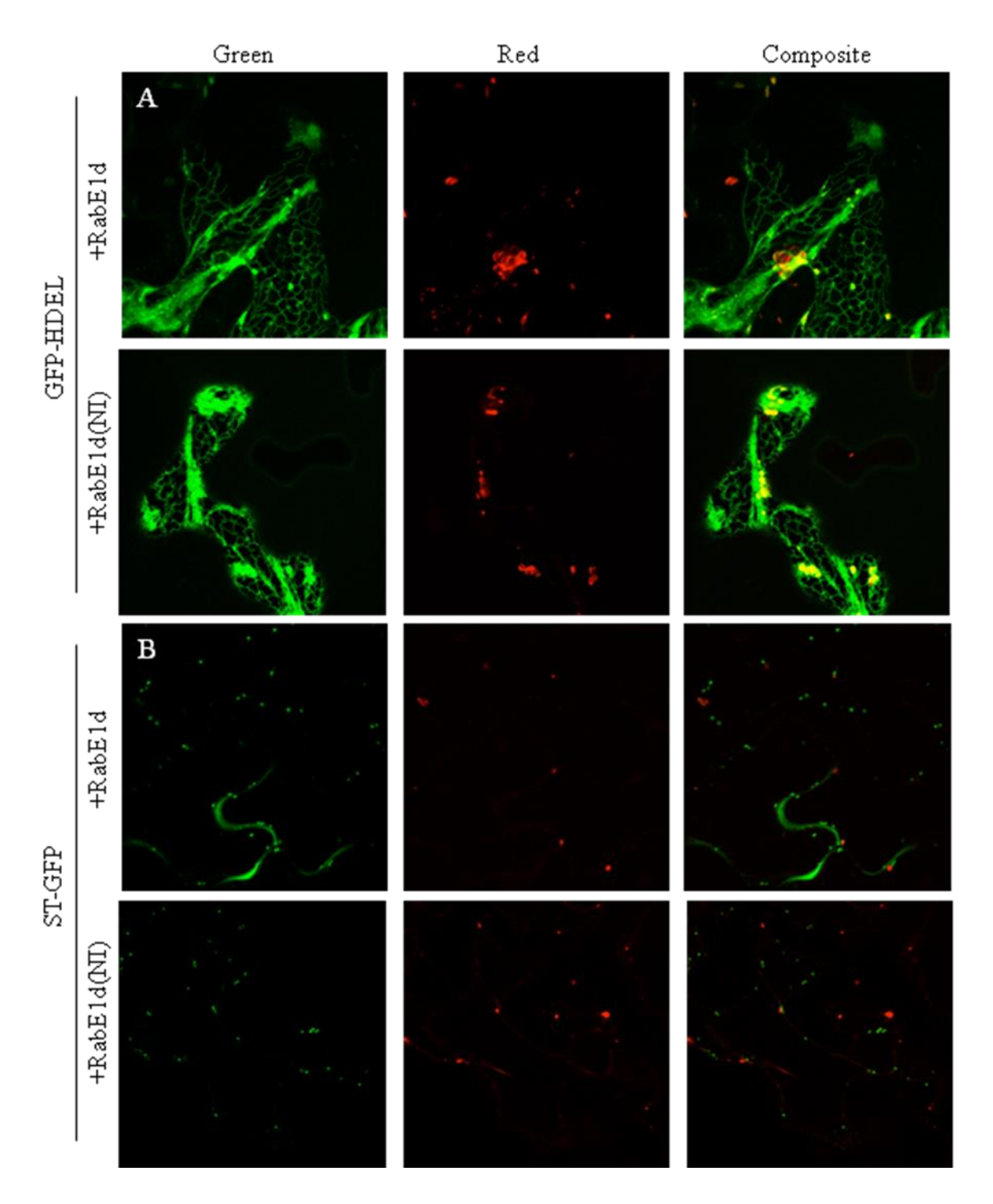


Figure 5: Localization of the 6K2-mCherry protein relative to the ER marker GFP-HDEL (A) and the Golgi marker ST-GFP (B) when co-expressed with either RabE1d or RabE1d-NI.

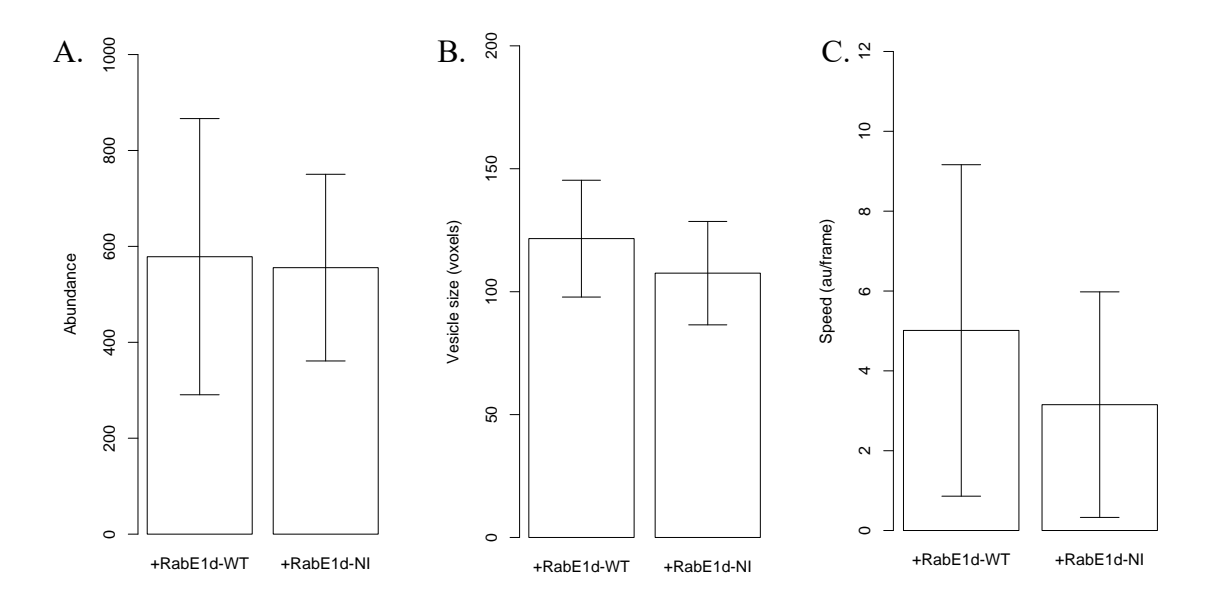
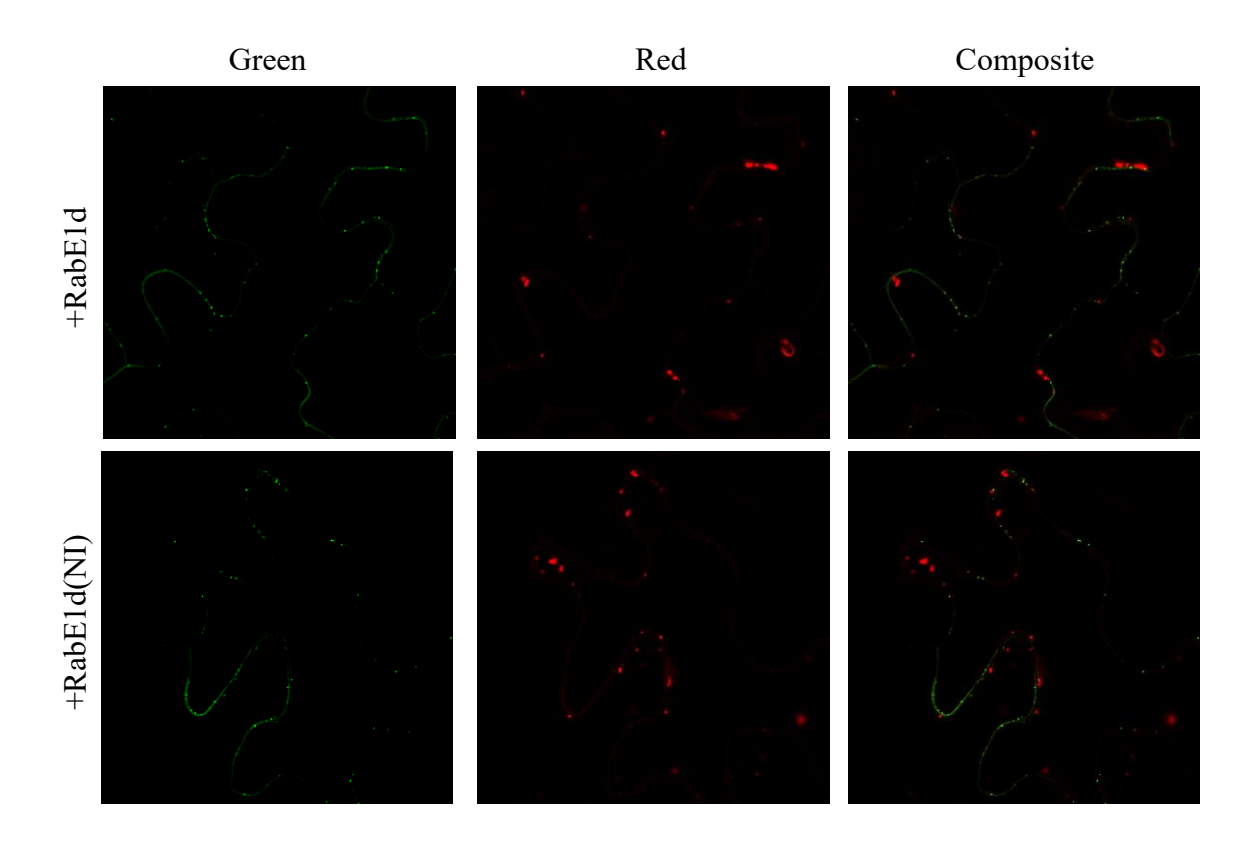


Figure 6: Quantification of 6K2-mCherry formed vesicles abundance (per single cell, A) (t-test n=10, p-value>0.05), average vesicle size (B) (t-test n=10, p-value>0.05) and average movement speed of the vesicular bodies (C) (t-test n=5, p-value>0.05).



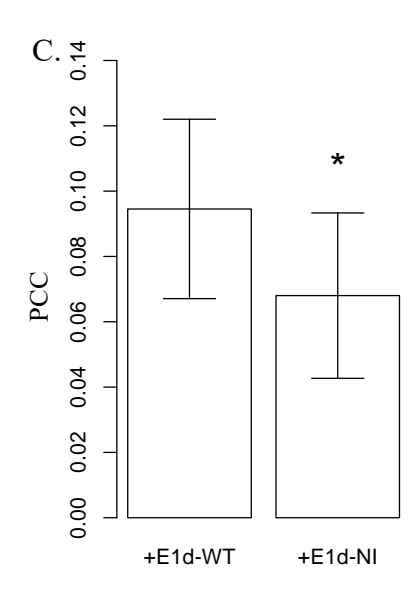


Figure 7: localization of 6K2-mCherry to PDLP1-GFP labeled PD during TuMV infection when co-expressed with either RabE1d (A) or the dominant negative RabE1d(NI) (B). (C) Quantification of the co-localization (PCC) between 6K2-mCherry and PDLP1-GFP during infection (t-test n=20, p-value<0.05).

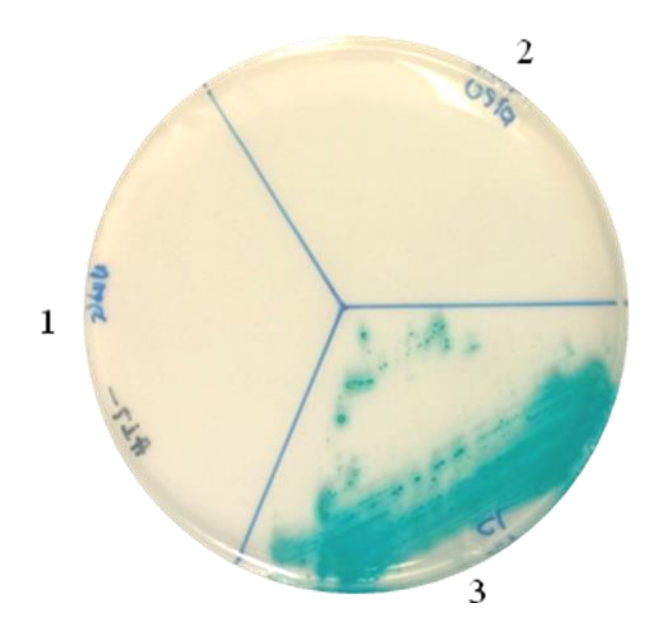


Figure 8: Y2H-SUS of PLV-Cub-6K2 and free NubG (1), PLV-Cub-6K2 and P3N-PIPO-NubG (2), and PLV-Cub-6K2 and CI-NubG (3). The mated cells were grown in SC-Leu-Trp-His + 3-AT.

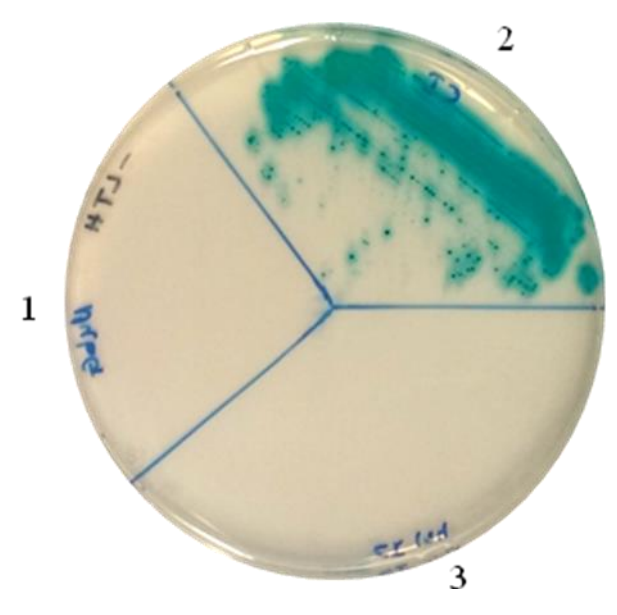


Figure 9: Y2H-SUS of PLV-Cub-6K2 and free NubG (1), PLV-Cub-6K2 and CI-NubG (2), and PLV-Cub-6K2 and CI-NubG(QS-124,126-AA) (3). The mated cells were grown in SC-Leu-Trp-His \pm 3-AT.

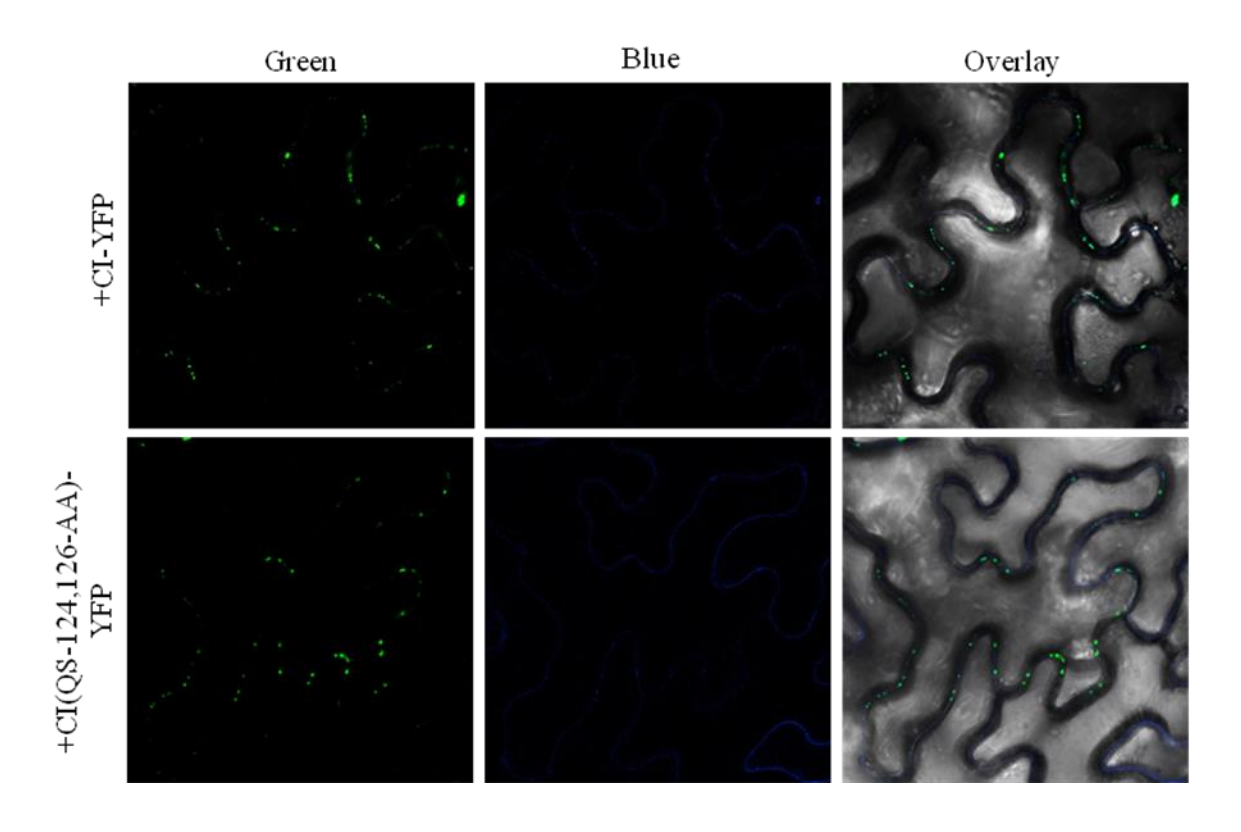


Figure 10: Localization of CI-YFP, and CI(QS-124,126-AA)-YFP when co-expressed with P3N-PIPO-CFP.

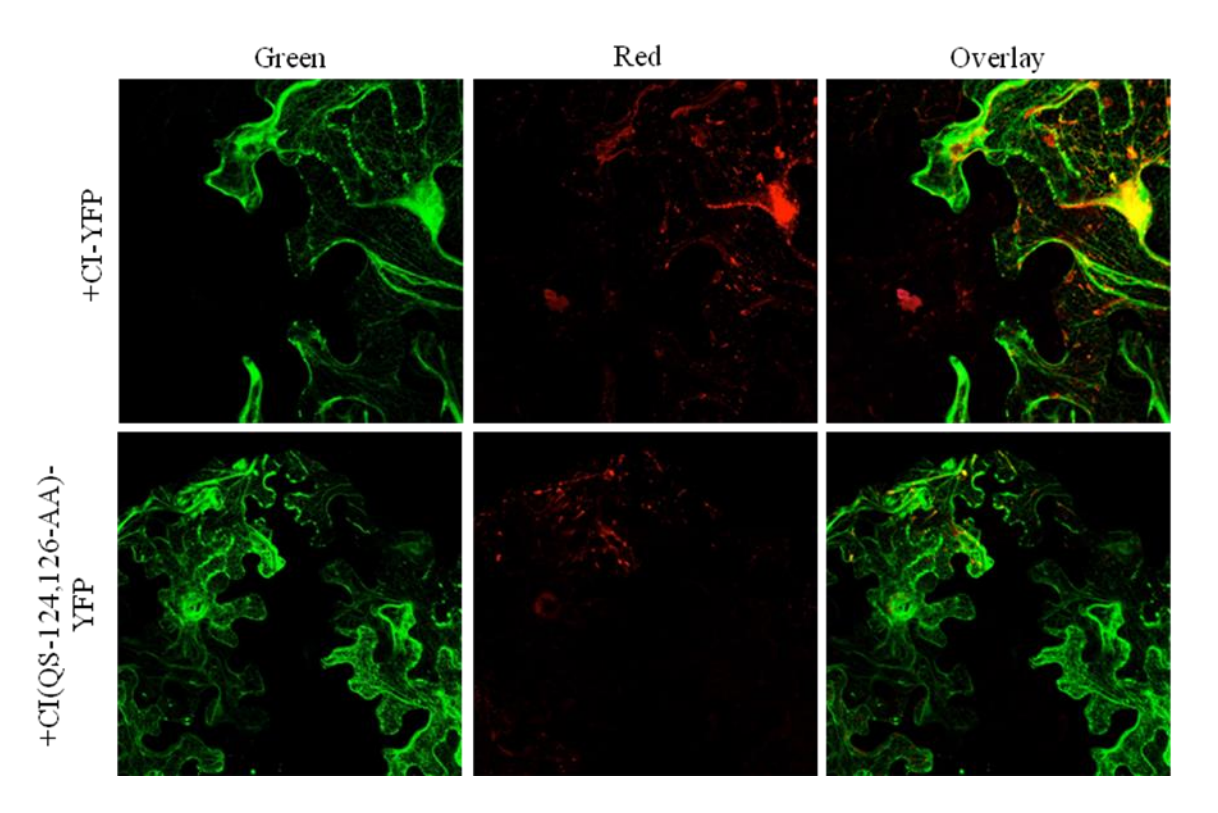


Figure 11: Intercellular movement of the 6K2-mCherry vesicles when co-expressed with P3N-PIPO-YFP and either CI-YFP, or CI(QS-124,126-AA)-YFP.

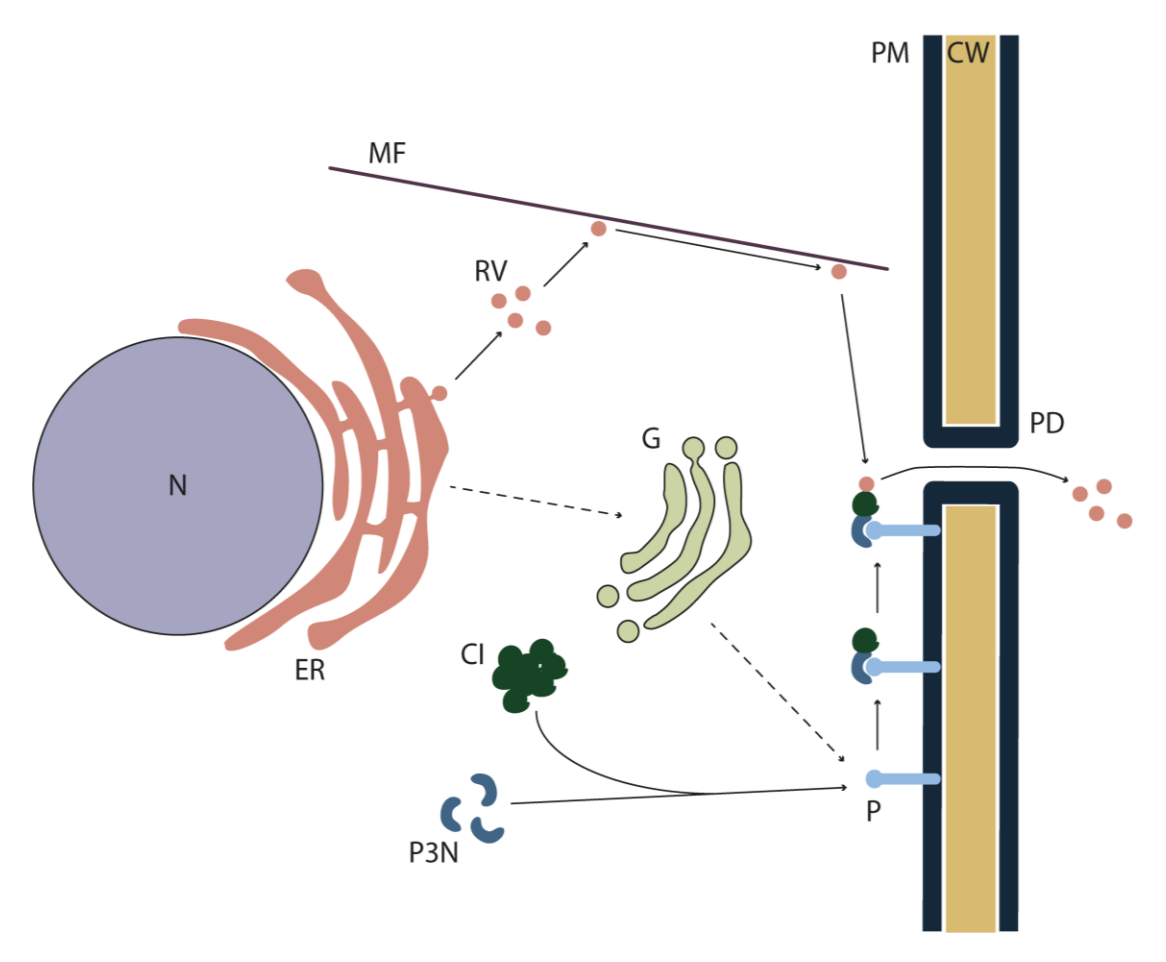


Figure 12: Schematic representation of the proposed mechanism for intercellular transport of TuMV replication vesicles. The dotted lines represent the ER-to-Golgi dependent transport of a yet unknown PD-associated protein (P) required for the correct targeting of P3N-PIPO to the PD. N: nucleus, ER: endoplasmic reticulum, RV: TuMV replication vesicles, MF: actin microfilaments, G: Golgi apparatus, PD: plasmodesmata, PM: plasma membrane, CW: cell wall, CI: TuMV cylindrical inclusion protein, P3N: TuMV P3N-PIPO protein.

Table 1: Primers used for the amplification (PCR) and site directed mutagenesis of the genes used in this study.

Primer name	Sequence
PCaP1-F	5' ATGGGTTACTGGAATTCCAAGGTTG 3'
PCaP1-R	5' AGGCTTTGGTGGTTCAGCCACTGGC 3'
P3N-PIPO-F	5' ATGGGAACAGAATGGGAGGACACTCATG 3'
P3N-PIPO-2-R	5' GTAGATAACTTT <u>C</u> TTTCCAAAATGG 3'
P3N-PIPO-2-F	5' CCATTTTGGAAAGAAAGTTATCTAC 3'
P3N-PIPO-R	5' CTCCGTTCGTAAGATGACATGACTG 3'
CI-F	5' ATGGACTCTCAATGATATAGAGGATGAC 3'
CI-R	5' TTGATGGTGAACTGCCTCAAGAGCTCC 3'
CI(QS124,126AA)-F	5' ATGGAACGGTGCCTGCGCCAACGCCTTGTGTACGTTTTCTG 3'
CI(QS124,126AA)-R	5' CAGAAAACGTACACAAGGCGTTGGCGCAGGCACCGTTCCAT 3'

Chapter 4:

Concluding Statements and Future Directions

4.1 Formation of TuMV replication vesicles

The TuMV 6K2 protein is the main viral protein involved in the formation of the replication vesicles of the virus. It has been indicated that the 6K2-mediated formation of replication vesicles is dependent on a functional COPII-COPI transport system. Here we show that 6K2 hijacks the COPII complex in order to induce the formation of TuMV replication vesicles. The interaction between the 6K2 and Sec24a plays a major role in this process. A new dual ER-export motif present in the N-terminal cytosolic portion of 6K2 was described. Interestingly both parts of the 6K2 ER-export signal are sufficient to mediate the recognition by the B-site of Sec24a. It is possible that a dual signal could have evolved to maximize the efficiency of the Sec24a recruitment to the ER by 6K2. 6K2 was able to interact with the Sar1-GEF Sec12 in a Y2H system. Sec12 is in charge of the activation of Sar1 which initiates the recruitment of the pre-budding complex of COPII [54, 83].

Since the complete disruption of the interaction between 6K2 and Sec24a does not abolish the 6K2-mediated vesicle formation, and that 6K2 is able to interact with Sec12 in a Y2H system, it is likely that this interaction would also play a role in the recruitment of the COPII complex by 6K2. Confirming the interaction between 6K2 and Sec12 and studying the involvement of Sec12 and even additional host factors in the 6K2-induced replication vesicle formation could provide a more complete mechanism for the formation of the TuMV replication complexes. In the Y2H system 6K2 is also able to physically interact with the COPI protein γ -COP, it would be interesting to confirm this interaction and then explore the connection between the COPI complex and the 6K2 formed vesicles.

This could be done by inserting point mutations in 6K2 that disrupt its interaction with γ -COP or Sec12, for example, and then visualize by confocal microscopy if the 6K2-mediated vesicle formation is altered when these interactions are abolished.

4.2 Minimal viral complex for the intercellular movement of TuMV replication vesicles In TuMV several viral proteins, P3N-PIPO, CI, HC-Pro and CP, have been shown to play a role in the cell-to-cell movement of this virus. In this study we show that the P3N-PIPO and CI proteins are necessary and sufficient to facilitate the intercellular movement of the 6K2-induced replication vesicles. The P3N-PIPO protein plays a role in modifying the SEL of PD, and it modulates the localization of the CI protein to the PD during viral infection [52]. Since 6K2 interacts directly with CI but not P3N-PIPO, we suggest that the 6K2 vesicles are docked to the modified plasmodesmata through the interaction with CI. This provides a previously unknown connection between the intercellular movement of the TuMV replication complexes and the modification of the PD mediated in part by P3N-PIPO. This idea was supported by the facts that disrupting the interaction between CI and 6K2 completely disrupts the intercellular movement of 6K2, and the inhibition of the correct localization of P3N-PIPO by the expression of the RabE1d dominant negative also inhibits the correct targeting of 6K2 to the PD, but does not seem to affect the formation of 6K2-induced replication vesicles or the localization of the PD localized

Even though these two proteins are sufficient to facilitate the intercellular movement of 6K2 vesicles, other viral proteins have been shown to be involved in the cell-to-cell spread of TuMV. For example, the CP has been shown to be involved in the cell-to-cell movement of TuMV and to accumulate at the PD together with P3N-PIPO and CI [52]. It

proteins PDLP1, PDCB1 or PCaP1.

would be interesting to study, using the infection-free system, additional viral factors involved in this process and to characterize the complete mechanism for the cell-to-cell spread during the TuMV infection. It would also be interesting to study host factors involved in this process.

We also showed that the RabE1d protein is involved in the localization of P3N-PIPO to PD. P3N-PIPO is not a transmembrane or membrane bound protein, thus its localization to the PD is likely mediated by a host protein. It has been shown that PCaP1, a PD localized cation binding protein, can act as an anchor for P3N-PIPO, however the localization of PCaP1, as well as other PD proteins such as PDLP1 or PDCB1 was not affected by the expression of the dominant negative RabE1d version. It would be interesting to study what host proteins involved in the localization of P3N-PIPO to arrive to a complete model for the targeting of this protein to PD. This could be done by first finding the PD-localized proteins whose correct localization can be disrupted by the coexpression of the RabE1d(NI) dominant negative. Then check which of those proteins is capable of directly interacting with P3N-PIPO and could explain its localization to PD. This would provide an interesting insight into the infectious process of potyviruses.

References

- 1. Nicolas, O. and J.-F. Laliberté, *The complete nucleotide sequence of turnip mosaic potyvirus RNA*. Journal of General Virology, 1992. **73**(11): p. 2785-2793.
- 2. Shattuck, V.I., et al., *The effect of turnip mosaic virus infection on the mineral content and storability of field-grown rutabaga*. Communications in Soil Science and Plant Analysis, 1989. **20**(5-6): p. 581-595.
- 3. Walsh, J.A. and C.E. Jenner, *Turnip mosaic virus and the quest for durable resistance*. Molecular Plant Pathology, 2002. **3**(5): p. 289-300.
- 4. Shattuck, V.I., *The biology, epidemiology, and control of turnip mosaic virus*, in *Horticultural Reviews*. 1992, John Wiley & Sons, Inc. p. 199-238.
- 5. Verchot, J., Wrapping membranes around plant virus infection. Curr Opin Virol, 2011. **1**(5): p. 388-95.
- 6. Laliberte, J.F. and H. Sanfacon, *Cellular remodeling during plant virus infection*. Annu Rev Phytopathol, 2010. **48**: p. 69-91.
- 7. Mackenzie, J., Wrapping things up about virus RNA replication. Traffic, 2005. **6**(11): p. 967-977.
- 8. Miller, S. and J. Krijnse-Locker, *Modification of intracellular membrane structures for virus replication*. Nat Rev Microbiol, 2008. **6**(5): p. 363-74.
- 9. Chung, B.Y.-W., et al., *An overlapping essential gene in the Potyviridae*. Proceedings of the National Academy of Sciences, 2008. **105**(15): p. 5897-5902.
- 10. Mavankal, G. and R.E. Rhoads, *In Vitro cleavage at or near the N-terminus of the helper component protein in the tobacco vein mottling virus polyprotein.* Virology, 1991. **185**(2): p. 721-731.
- 11. Verchot, J., E.V. Koonin, and J.C. Carrington, *The 35-kDa protein from the N-terminus of the potyviral polyprotein functions as a third virus-encoded proteinase.* Virology, 1991. **185**(2): p. 527-535.
- 12. Carrington, J.C., et al., *Internal cleavage and trans-proteolytic activities of the VPg-proteinase (NIa) of tobacco etch potyvirus in vivo*. Journal of Virology, 1993. **67**(12): p. 6995-7000.
- 13. Beauchemin, C., N. Boutet, and J.F. Laliberte, *Visualization of the interaction between the precursors of VPg, the viral protein linked to the genome of turnip mosaic virus, and the translation eukaryotic initiation factor iso 4E in Planta.* J Virol, 2007. **81**(2): p. 775-82.
- 14. Schaad, M.C., P.E. Jensen, and J.C. Carrington, Formation of plant RNA virus replication complexes on membranes: role of an endoplasmic reticulum-targeted viral protein. Embo Journal, 1997. **16**(13): p. 4049-59.
- 15. Grangeon, R., et al., *Impact on the endoplasmic reticulum and Golgi apparatus of turnip mosaic virus infection.* J Virol, 2012. **86**(17): p. 9255-65.
- 16. Cotton, S., et al., Turnip mosaic virus RNA replication complex vesicles are mobile, align with microfilaments, and are each derived from a single viral genome. J Virol, 2009. **83**(20): p. 10460-71.
- 17. Dufresne, P.J., et al., *Heat shock 70 protein interaction with Turnip mosaic virus RNA-dependent RNA polymerase within virus-induced membrane vesicles.* Virology, 2008. **374**(1): p. 217-27.

- 18. Thivierge, K., et al., Eukaryotic elongation factor 1A interacts with Turnip mosaic virus RNA-dependent RNA polymerase and VPg-Pro in virus-induced vesicles. Virology, 2008. 377(1): p. 216-25.
- 19. Beauchemin, C. and J.F. Laliberte, *The poly(A) binding protein is internalized in virus-induced vesicles or redistributed to the nucleolus during turnip mosaic virus infection*. J Virol, 2007. **81**(20): p. 10905-13.
- 20. Leonard, S., et al., *Interaction of VPg-Pro of turnip mosaic virus with the translation initiation factor 4E and the poly(A)-binding protein in planta.* J Gen Virol, 2004. **85**(Pt 4): p. 1055-63.
- 21. Craig, E.A., et al., 2 Cytosolic hsp70s of <u>Saccharomyces cerevisiae</u>: roles in protein synthesis, protein translocation, proteolysis, and regulation. 1994. 1994.
- 22. Mayer, M.P. and B. Bukau, *Hsp70 chaperones: cellular functions and molecular mechanism*. Cell Mol Life Sci, 2005. **62**(6): p. 670-84.
- 23. Brown, G., et al., Evidence for an association between heat shock protein 70 and the respiratory syncytial virus polymerase complex within lipid-raft membranes during virus infection. Virology, 2005. **338**(1): p. 69-80.
- 24. Glotzer, J.B., et al., *Activation of heat-shock response by an adenovirus is essential for virus replication*. Nature, 2000. **407**(6801): p. 207-11.
- 25. Hu, J., et al., Requirement of heat shock protein 90 for human hepatitis B virus reverse transcriptase function. J Virol, 2004. **78**(23): p. 13122-31.
- 26. Kampmueller, K.M. and D.J. Miller, *The cellular chaperone heat shock protein* 90 facilitates Flock House virus RNA replication in <u>Drosophila</u> cells. J Virol, 2005. **79**(11): p. 6827-37.
- 27. Momose, F., et al., *Identification of Hsp90 as a stimulatory host factor involved in influenza virus RNA synthesis.* J Biol Chem, 2002. **277**(47): p. 45306-14.
- 28. Grangeon, R., et al., 6K2-induced vesicles can move cell to cell during turnip mosaic virus infection. Front Microbiol, 2013. 4: p. 351.
- 29. Wei, T. and A. Wang, Biogenesis of cytoplasmic membranous vesicles for plant potyvirus replication occurs at endoplasmic reticulum exit sites in a COPI- and COPII-dependent manner. J Virol, 2008. **82**(24): p. 12252-64.
- 30. Nebenfuhr, A., C. Ritzenthaler, and D.G. Robinson, *Brefeldin A: deciphering an enigmatic inhibitor of secretion*. Plant Physiol, 2002. **130**(3): p. 1102-8.
- 31. Baluska, F., et al., *Latrunculin B-induced plant dwarfism: Plant cell elongation is F-actin-dependent.* Developmental Biology, 2001. **231**(1): p. 113-124.
- Wan, J., et al., *Turnip mosaic virus moves systemically through both phloem and xylem as membrane-associated complexes*. Plant Physiol, 2015. **167**(4): p. 1374-88.
- 33. Li, X.H., et al., Functions of the tobacco etch virus RNA polymerase (NIb): subcellular transport and protein-protein interaction with VPg/proteinase (NIa). Journal of Virology, 1997. **71**(2): p. 1598-1607.
- 34. Fellers, J., et al., *In vitro interactions between a potyvirus-encoded, genomelinked protein and RNA-dependent RNA polymerase.* Journal of General Virology, 1998. **79**(8): p. 2043-2049.
- 35. Léonard, S., et al., *Interaction of VPg-Pro of Turnip mosaic virus with the translation initiation factor 4E and the poly(A)-binding protein in planta*. Journal of General Virology, 2004. **85**(4): p. 1055-1063.

- 36. Puustinen, P. and K. Makinen, *Uridylylation of the potyvirus VPg by viral replicase NIb correlates with the nucleotide binding capacity of VPg.* J Biol Chem, 2004. **279**(37): p. 38103-10.
- 37. Fernández, A., S. Laín, and J.A. García, RNA helicase activity of the plum pox potyvirus CI protein expressed in <u>Escherichia coli</u>. Mapping of an RNA binding domain. Nucleic Acids Research, 1995. **23**(8): p. 1327-1332.
- 38. Lain, S., J.L. Riechmann, and J.A. Garciá, *RNA helicase: a novel activity associated with a protein encoded by a positive strand RNA virus*. Nucleic Acids Research, 1990. **18**(23): p. 7003-7006.
- 39. Laín, S., et al., Novel catalytic activity associated with positive-strand RNA virus infection: nucleic acid-stimulated ATPase activity of the plum pox potyvirus helicaselike protein. Journal of Virology, 1991. **65**(1): p. 1-6.
- 40. Eagles, R.M., et al., Characterization of NTPase, RNA-binding and RNA-helicase activities of the cytoplasmic inclusion protein of tamarillo mosaic potyvirus. European Journal of Biochemistry, 1994. **224**(2): p. 677-684.
- 41. Carrington, J.C., P.E. Jensen, and M.C. Schaad, *Genetic evidence for an essential role for potyvirus CI protein in cell-to-cell movement*. Plant J, 1998. **14**(4): p. 393-400.
- 42. Kekarainen, T., H. Savilahti, and J.P.T. Valkonen, Functional genomics on potato virus a: virus genome-wide map of sites essential for virus propagation. Genome Research, 2002. **12**(4): p. 584-594.
- 43. Klein, P.G., et al., *Mutational analysis of the tobacco vein mottling virus genome.* Virology, 1994. **204**(2): p. 759-769.
- 44. Benitez-Alfonso, Y., et al., *Plasmodesmata: gateways to local and systemic virus infection*. Molecular Plant-Microbe Interactions, 2010. **23**(11): p. 1403-1412.
- 45. Niehl, A. and M. Heinlein, *Cellular pathways for viral transport through plasmodesmata*. Protoplasma, 2011. **248**(1): p. 75-99.
- 46. Schoelz, J.E., P.A. Harries, and R.S. Nelson, *Intracellular transport of plant viruses: finding the door out of the cell.* Mol Plant, 2011. **4**(5): p. 813-31.
- 47. Heinlein, M., *Plasmodesmata: channels for viruses on the move*, in *plasmodesmata*, M. Heinlein, Editor. 2015, Springer New York. p. 25-52.
- 48. Hipper, C., et al., *Viral and cellular factors involved in phloem transport of plant viruses.* Frontiers in Plant Science, 2013. **4**.
- 49. Vuorinen, A.L., J. Kelloniemi, and J.P.T. Valkonen, *Why do viruses need phloem for systemic invasion of plants?* Plant Science, 2011. **181**(4): p. 355-363.
- 50. Lucas, W.J., Plant viral movement proteins: Agents for cell-to-cell trafficking of viral genomes. Virology, 2006. **344**(1): p. 169-184.
- 51. Vijayapalani, P., et al., Interaction of the trans-frame potyvirus protein P3N-PIPO with host protein PCaP1 facilitates potyvirus movement. PLoS Pathog, 2012. **8**(4): p. e1002639.
- 52. Wei, T., et al., Formation of complexes at plasmodesmata for potyvirus intercellular movement is mediated by the viral protein P3N-PIPO. PLoS Pathog, 2010. **6**(6): p. e1000962.
- 53. Lucas, W.J., B.K. Ham, and J.Y. Kim, *Plasmodesmata bridging the gap between neighboring plant cells*. Trends Cell Biol, 2009. **19**(10): p. 495-503.

- 54. Lee, M.C. and E.A. Miller, *Molecular mechanisms of COPII vesicle formation*. Semin Cell Dev Biol, 2007. **18**(4): p. 424-34.
- 55. Brandizzi, F. and C. Barlowe, *Organization of the ER-Golgi interface for membrane traffic control*. Nat Rev Mol Cell Biol, 2013. **14**(6): p. 382-392.
- 56. Spector, I., et al., Latrunculins—novel marine macrolides that disrupt microfilament organization and affect cell growth: I. Comparison with cytochalasin D. Cell Motility and the Cytoskeleton, 1989. **13**(3): p. 127-144.
- 57. Spector, I., et al., *Latrunculins: novel marine toxins that disrupt microfilament organization in cultured cells.* Science, 1983. **219**(4584): p. 493-495.
- 58. Amari, K., et al., Myosins VIII and XI play distinct roles in reproduction and transport of tobacco mosaic virus. PLoS Pathog, 2014. 10(10): p. e1004448.
- 59. Gómez de Cedrón, M., et al., Genetic analysis of the function of the plum pox virus CI RNA helicase in virus movement. Virus Research, 2006. **116**(1–2): p. 136-145.
- 60. Deng, P., Z. Wu, and A. Wang, *The multifunctional protein CI of potyviruses plays interlinked and distinct roles in viral genome replication and intercellular movement.* Virology Journal, 2015. **12**(1): p. 1-11.
- 61. López, L., et al., *Identification of an N-terminal domain of the plum pox potyvirus CI RNA helicase involved in self-interaction in a yeast two-hybrid system.* Journal of General Virology, 2001. **82**(3): p. 677-686.
- 62. Guo, B., J. Lin, and K. Ye, Structure of the autocatalytic cysteine protease domain of potyvirus helper-component proteinase. Journal of Biological Chemistry, 2011. **286**(24): p. 21937-21943.
- 63. Plisson, C., et al., Structural characterization of HC-Pro, a plant virus multifunctional protein. Journal of Biological Chemistry, 2003. **278**(26): p. 23753-23761.
- Wang, R.Y., et al., Role of the helper component in vector-specific transmission of potyviruses. Journal of General Virology, 1998. **79**(6): p. 1519-1524.
- 65. Maia, I.G., A.-L. Haenni, and F. Bernardi, *Potyviral HC-Pro: a multifunctional protein*. Journal of General Virology, 1996. **77**(7): p. 1335-1341.
- 66. Peng, Y.H., et al., Mutations in the HC-Pro gene of zucchini yellow mosaic potyvirus: effects on aphid transmission and binding to purified virions. Journal of General Virology, 1998. **79**(4): p. 897-904.
- 67. Yap, Y.-K., J. Duangjit, and S. Panyim, *N-terminal of Papaya ringspot virus type-W (PRSV-W) helper component proteinase (HC-Pro) is essential for PRSV systemic infection in zucchini*. Virus Genes, 2009. **38**(3): p. 461-467.
- 68. Blanc, S., et al., A Specific interaction between coat protein and helper component correlates with aphid transmission of a potyvirus. Virology, 1997. **231**(1): p. 141-147.
- 69. Dombrovsky, A., et al., Aphid transmission of a potyvirus depends on suitability of the helper component and the N terminus of the coat protein. Archives of Virology, 2005. **150**(2): p. 287-298.
- 70. Urcuqui-Inchima, S., et al., *Deletion mapping of the potyviral Helper Component-Proteinase reveals two regions involved in rna binding.* Virology, 2000. **268**(1): p. 104-111.

- 71. Urcuqui-Inchima, S., A.L. Haenni, and F. Bernardi, *Potyvirus proteins: a wealth of functions*. Virus Res, 2001. **74**(1-2): p. 157-75.
- 72. Anindya, R. and H.S. Savithri, *Surface-exposed amino- and carboxy-terminal residues are crucial for the initiation of assembly in Pepper vein banding virus: a flexuous rod-shaped virus.* Virology, 2003. **316**(2): p. 325-336.
- 73. Ivanov, K.I., et al., *Phosphorylation of the potyvirus capsid protein by protein kinase CK2 and its relevance for virus infection*. The Plant Cell, 2003. **15**(9): p. 2124-2139.
- 74. Verchot, J. and J.C. Carrington, *Debilitation of plant potyvirus infectivity by P1 proteinase-inactivating mutations and restoration by second-site modifications*. Journal of Virology, 1995. **69**(3): p. 1582-90.
- 75. Verchot, J. and J.C. Carrington, Evidence that the potyvirus P1 proteinase functions in trans as an accessory factor for genome amplification. Journal of Virology, 1995. **69**(6): p. 3668-3674.
- 76. Soumounou, Y. and J.-F. Laliberté, *Nucleic acid-binding properties of the P1 protein of turnip mosaic potyvirus produced in <u>Escherichia coli</u>. Journal of General Virology, 1994. 75(10): p. 2567-2573.*
- 77. Jenner, C.E., et al., The dual role of the potyvirus P3 protein of turnip mosaic virus as a symptom and avirulence determinant in Brassicas. Molecular Plant-Microbe Interactions, 2003. **16**(9): p. 777-784.
- 78. Rodríguez-Cerezo, E., et al., Association of the non-structural P3 viral protein with cylindrical inclusions in potyvirus-infected cells. Journal of General Virology, 1993. 74(9): p. 1945-1949.
- 79. Cui, X., et al., The Tobacco etch virus P3 protein forms mobile inclusions via the early secretory pathway and traffics along actin microfilaments. Virology, 2010. **397**(1): p. 56-63.
- 80. Riechmann, J.L., M.T. Cervera, and J.A. García, *Processing of the plum pox virus polyprotein at the P3-6K1 junction is not required for virus viability*. Journal of General Virology, 1995. **76**(4): p. 951-956.
- 81. Jiang, J., et al., The vesicle-forming 6K2 protein of turnip mosaic virus interacts with the COPII coatomer Sec24a for viral systemic infection. J Virol, 2015. **89**(13): p. 6695-710.
- 82. Waltermann, A. and E. Maiss, *Detection of 6K1 as a mature protein of 6kDa in plum pox virus-infected Nicotiana benthamiana*. Journal of General Virology, 2006. **87**(8): p. 2381-2386.
- 83. Marti, L., et al., *COPII-mediated traffic in plants*. Trends Plant Sci, 2010. **15**(9): p. 522-8.
- 84. Bickford, L.C., E. Mossessova, and J. Goldberg, *A structural view of the COPII vesicle coat*. Curr Opin Struct Biol, 2004. **14**(2): p. 147-53.
- 85. Miller, E., et al., Cargo selection into COPII vesicles is driven by the Sec24p subunit. Embo Journal, 2002. **21**(22): p. 6105-6113.
- 86. Barlowe, C., Signals for COPII-dependent export from the ER: what's the ticket out? Trends in Cell Biology, 2003. **13**(6): p. 295-300.
- 87. Miller, E.A., et al., Multiple cargo binding sites on the COPII subunit Sec24p ensure capture of diverse membrane proteins into transport vesicles. Cell, 2003. 114(4): p. 497-509.

- 88. Mossessova, E., L.C. Bickford, and J. Goldberg, *SNARE selectivity of the COPII coat*. Cell, 2003. **114**(4): p. 483-95.
- 89. Antonny, B., et al., *Dynamics of the COPII coat with GTP and stable analogues*. Nat Cell Biol, 2001. **3**(6): p. 531-7.
- 90. Sato, K. and A. Nakano, Dissection of COPII subunit-cargo assembly and disassembly kinetics during Sar1p-GTP hydrolysis. Nat Struct Mol Biol, 2005. 12(2): p. 167-74.
- 91. Eugster, A., et al., COP I domains required for coatomer integrity, and novel interactions with ARF and ARF-GAP. The EMBO Journal, 2000. **19**(15): p. 3905-3917.
- 92. Szul, T. and E. Sztul, *COPII and COPI traffic at the ER-Golgi interface*. Physiology (Bethesda), 2011. **26**(5): p. 348-64.
- 93. Nie, Z. and P.A. Randazzo, *Arf GAPs and membrane traffic*. Journal of Cell Science, 2006. **119**(7): p. 1203-1211.
- 94. Traub, L.M. and S. Kornfeld, *The trans-Golgi network: a late secretory sorting station*. Curr Opin Cell Biol, 1997. **9**(4): p. 527-33.
- 95. Clague, M.J. and S. Urbe, *The interface of receptor trafficking and signalling*. J Cell Sci, 2001. **114**(Pt 17): p. 3075-81.
- 96. Gruenberg, J. and F.R. Maxfield, *Membrane transport in the endocytic pathway*. Curr Opin Cell Biol, 1995. **7**(4): p. 552-63.
- 97. Gorvel, J.P., et al., *Rab5 controls early endosome fusion in vitro*. Cell, 1991. **64**(5): p. 915-25.
- 98. Rink, J., et al., *Rab conversion as a mechanism of progression from early to late endosomes*. Cell, 2005. **122**(5): p. 735-49.
- 99. Grant, B.D. and J.G. Donaldson, *Pathways and mechanisms of endocytic recycling*. Nat Rev Mol Cell Biol, 2009. **10**(9): p. 597-608.
- 100. Bonifacino, J.S. and B.S. Glick, *The mechanisms of vesicle budding and fusion*. Cell, 2004. **116**(2): p. 153-66.
- 101. Dettmer, J., et al., Vacuolar H+-ATPase activity is required for endocytic and secretory trafficking in Arabidopsis. Plant Cell, 2006. **18**(3): p. 715-30.
- 102. Kang, B.H., et al., Electron tomography of RabA4b- and PI-4Kbeta1-labeled trans Golgi network compartments in Arabidopsis. Traffic, 2011. **12**(3): p. 313-29.
- 103. Qi, X., et al., A specific role for <u>Arabidopsis</u> TRAPPII in post-Golgi trafficking that is crucial for cytokinesis and cell polarity. Plant J, 2011. **68**(2): p. 234-48.
- 104. Preuss, M.L., et al., A role for the RabA4b effector protein PI-4Kbeta1 in polarized expansion of root hair cells in <u>Arabidopsis thaliana</u>. J Cell Biol, 2006. **172**(7): p. 991-8.
- 105. Szumlanski, A.L. and E. Nielsen, *The Rab GTPase RabA4d regulates pollen tube tip growth in <u>Arabidopsis thaliana</u>. Plant Cell, 2009. 21(2): p. 526-44.*
- 106. Ueda, T., et al., *Ara6, a plant-unique novel type Rab GTPase, functions in the endocytic pathway of <u>Arabidopsis thaliana</u>. Embo Journal, 2001. 20(17): p. 4730-4741.*
- 107. Spitzer, C., et al., *The ESCRT-related CHMP1A and B proteins mediate multivesicular body sorting of auxin carriers in <u>Arabidopsis</u> and are required for plant development. Plant Cell, 2009. 21(3): p. 749-66.*

- 108. Choi, S.-w., et al., *RABA members act in distinct steps of subcellular trafficking of the FLAGELLIN SENSING2 Receptor.* The Plant Cell, 2013. **25**(3): p. 1174-1187.
- 109. Feraru, E., et al., *BEX5/RabA1b* regulates trans-Golgi network-to-plasma membrane protein trafficking in <u>Arabidopsis</u>. The Plant Cell, 2012. **24**(7): p. 3074-3086.
- 110. Zheng, H., et al., A Rab-E GTPase mutant acts downstream of the Rab-D subclass in biosynthetic membrane traffic to the plasma membrane in tobacco leaf epidermis. The Plant Cell, 2005. 17(7): p. 2020-2036.
- 111. Maule, A.J., *Plasmodesmata: structure, function and biogenesis*. Curr Opin Plant Biol, 2008. **11**(6): p. 680-6.
- 112. Bayer, E., C.L. Thomas, and A.J. Maule, *Plasmodesmata in <u>Arabidopsis thaliana</u> suspension cells*. Protoplasma, 2004. **223**(2-4): p. 93-102.
- 113. Burgess, J., *Observations on structure and differentiation in plasmodesmata*. Protoplasma, 1971. **73**(1): p. 83-95.
- 114. Overall, R.L. and L.M. Blackman, *A model of the macromolecular structure of plasmodesmata*. Trends in Plant Science, 1996. **1**(9): p. 307-311.
- 115. Kragler, F., *Plasmodesmata: intercellular tunnels facilitating transport of macromolecules in plants.* Cell Tissue Res, 2013. **352**(1): p. 49-58.
- 116. Levy, A., D. Guenoune-Gelbart, and B.L. Epel, *beta-1,3-Glucanases: Plasmodesmal gate keepers for intercellular communication.* Plant Signal Behav, 2007. **2**(5): p. 404-7.
- 117. Vaten, A., et al., *Callose biosynthesis regulates symplastic trafficking during root development.* Dev Cell, 2011. **21**(6): p. 1144-55.
- 118. Guseman, J.M., et al., *Dysregulation of cell-to-cell connectivity and stomatal patterning by loss-of-function mutation in <u>Arabidopsis</u> chorus (glucan synthase-like 8). Development, 2010. 137(10): p. 1731-41.*
- 119. De Storme, N. and D. Geelen, *Callose homeostasis at plasmodesmata: molecular regulators and developmental relevance.* Front Plant Sci, 2014. **5**: p. 138.
- 120. Chen, X.Y. and J.Y. Kim, *Callose synthesis in higher plants*. Plant Signal Behav, 2009. **4**(6): p. 489-92.
- 121. Zavaliev, R., et al., *Biology of callose (beta-1,3-glucan) turnover at plasmodesmata*. Protoplasma, 2011. **248**(1): p. 117-30.
- 122. Kumar, D., et al., *Cell-to-cell movement of viruses via plasmodesmata*. J Plant Res, 2015. **128**(1): p. 37-47.
- 123. Kasteel, D.T., et al., *The movement proteins of cowpea mosaic virus and cauliflower mosaic virus induce tubular structures in plant and insect cells.* J Gen Virol, 1996. **77 (Pt 11)**: p. 2857-64.
- 124. Wellink, J., et al., The cowpea mosaic virus M RNA-encoded 48-kilodalton protein is responsible for induction of tubular structures in protoplasts. J Virol, 1993. **67**(6): p. 3660-4.
- 125. Nairn, J.C., D.J. Lewandowski, and J.K. Burns, *Genetics and expression of two pectinesterase genes in <u>Valencia orange</u>. Physiologia Plantarum, 1998. 102(2): p. 226-235.*
- 126. Pressey, R., Role of pectinesterase in pH-Dependent interactions between pea cell wall polymers. Plant Physiol, 1984. **76**(2): p. 547-9.

- 127. Chen, M.H., et al., Interaction between the tobacco mosaic virus movement protein and host cell pectin methylesterases is required for viral cell-to-cell movement. EMBO J, 2000. 19(5): p. 913-20.
- 128. Grefen, C., S. Lalonde, and P. Obrdlik, Split-ubiquitin system for identifying protein-protein interactions in membrane and full-length proteins. Curr Protoc Neurosci, 2007. Chapter 5: p. Unit 5 27.
- 129. Jiang, J. and J.F. Laliberte, *The genome-linked protein VPg of plant viruses-a protein with many partners*. Curr Opin Virol, 2011. **1**(5): p. 347-54.
- 130. Wei, T., et al., Sequential recruitment of the endoplasmic reticulum and chloroplasts for plant potyvirus replication. J Virol, 2010. **84**(2): p. 799-809.
- 131. Heinlein, M., *Plant virus replication and movement*. Virology, 2015. **479-480C**: p. 657-671.
- 132. Hwang, I. and D.G. Robinson, *Transport vesicle formation in plant cells*. Curr Opin Plant Biol, 2009. **12**(6): p. 660-9.
- 133. Pagant, S., et al., Sec24 is a coincidence detector that simultaneously binds two signals to drive ER export. Current Biology, 2015. **25**(4): p. 403-412.
- 134. Giraudo, C.G. and H.J.F. Maccioni, *Endoplasmic reticulum export of glycosyltransferases depends on interaction of a cytoplasmic dibasic motif with Sar1*. Molecular Biology of the Cell, 2003. **14**(9): p. 3753-3766.
- 135. Chatre, L., et al., A novel di-acidic motif facilitates ER export of the syntaxin SYP31. Journal of Experimental Botany, 2009. **60**(11): p. 3157-3165.
- 136. Bonifacino, J.S. and B.S. Glick, *The Mechanisms of vesicle budding and fusion*. Cell, 2004. **116**(2): p. 153-166.
- 137. Kumichel, A., K. Kapp, and E. Knust, *A conserved di-basic motif of <u>Drosophila</u> crumbs contributes to efficient ER export*. Traffic, 2015. **16**(6): p. 604-616.
- 138. Agbeci, M., et al., Contribution of host intracellular transport machineries to intercellular movement of turnip mosaic virus. PLoS Pathog, 2013. 9(10): p. e1003683.
- 139. Faso, C., et al., A missense mutation in the <u>Arabidopsis</u> COPII coat protein Sec24A induces the formation of clusters of the endoplasmic reticulum and Golgi apparatus. Plant Cell, 2009. **21**(11): p. 3655-71.
- 140. Hofgen, R. and L. Willmitzer, *Storage of competent cells for <u>Agrobacterium</u> transformation*. Nucleic Acids Research, 1988. **16**(20): p. 9877.
- 141. Sparkes, I.A., et al., *Rapid, transient expression of fluorescent fusion proteins in tobacco plants and generation of stably transformed plants.* Nat. Protocols, 2006. **1**(4): p. 2019-2025.
- 142. Brennan, M.B. and K. Struhl, *Mechanisms of increasing expression of a yeast gene in Escherichia coli*. Journal of Molecular Biology, 1980. **136**(3): p. 333-338.
- 143. Grangeon, R., et al., 6K2-induced vesicles can move cell to cell during turnip mosaic virus infection. Frontiers in Microbiology, 2013. 4.
- 144. Brandenburg, B. and X. Zhuang, *Virus trafficking learning from single-virus tracking*. Nat Rev Microbiol, 2007. **5**(3): p. 197-208.
- 145. Ritzenthaler, C., Parallels and distinctions in the direct cell-to-cell spread of the plant and animal viruses. Curr Opin Virol, 2011. 1(5): p. 403-9.

- 146. Ueki, S. and V. Citovsky, To gate, or not to gate: regulatory mechanisms for intercellular protein transport and virus movement in plants. Mol Plant, 2011. 4(5): p. 782-93.
- 147. Speth, E.B., et al., Subcellular localization and functional analysis of the Arabidopsis GTPase RabE. Plant Physiology, 2009. **149**(4): p. 1824-1837.
- 148. Thomas, C.L., et al., Specific targeting of a plasmodesmal protein affecting cell-to-cell communication. PLoS Biol, 2008. **6**(1): p. 180-190.
- 149. Simpson, C., et al., An <u>Arabidopsis</u> GPI-Anchor plasmodesmal neck protein with callose binding activity and potential to regulate cell-to-cell trafficking. The Plant Cell, 2009. **21**(2): p. 581-594.
- 150. Earley, K.W., et al., *Gateway-compatible vectors for plant functional genomics and proteomics*. The Plant Journal, 2006. **45**(4): p. 616-629.
- 151. Amari, K., et al., A family of plasmodesmal proteins with receptor-like properties for plant viral movement proteins. PLoS Pathog, 2010. **6**(9): p. e1001119.
- 152. Amari, K., et al., *Tubule-guided cell-to-cell movement of a plant virus requires class XI myosin motors*. PLoS Pathog, 2011. 7(10): p. e1002327.
- 153. Zheng, H., et al., A GFP-based assay reveals a role for RHD3 in transport between the endoplasmic reticulum and Golgi apparatus. Plant J, 2004. 37(3): p. 398-414.
- 154. Bolte, S. and F.P. Cordelieres, *A guided tour into subcellular colocalization analysis in light microscopy*. Journal of Microscopy, 2006. **224**(3): p. 213-232.
- 155. Meijering, E., O. Dzyubachyk, and I. Smal, *Chapter nine methods for cell and particle tracking*, in *methods in enzymology*, P.M. conn, Editor. 2012, Academic Press. p. 183-200.